DOI: 10.1002/ejic.201000111

A Structural Investigation of Trivalent and Divalent Rare Earth Thiocyanate Complexes Synthesised by Redox Transmetallation

Jacinta M. Bakker,[a] Glen B. Deacon,*[a] Craig M. Forsyth,[a] Peter C. Junk,*[a] and Michal Wiecko[a]

Keywords: Rare earths / N ligands / Ether ligands / Redox chemistry / Transmetallation / Solid-state structures

A wide range of reactive trivalent and divalent rare earth thiocyanate complexes with 1,2-dimethoxyethane (dme), tetrahydrofuran (thf) and acetonitrile namely $[RE(NCS)_3(dme)_3]$ [RE = La (**1a**), Nd (**1b**)], $[RE(NCS)_3(dme)_2(\mu\text{-}dme)_{0.5}]_2$ [RE = Dy (**1d**), Er (**1e**)], $[RE(NCS)_3(thf)_4]_2$ [RE = Y (**3a**), La (**3b**), Nd (**3c**), Sm (**3d**), Dy (**3e**), Ho (**3f**)], $[Ca(NCS)_2(dme)_3]$ [**rac**-(**4a**)], $[RE(NCS)_2(dme)_3]$ (RE = Sm (*rac*-**4b**), Eu (*rac*-**4c**), $[Ca(Yb)(NCS)_2(NCMe)_5]\cdot NCMe$ [Ca (**6a**), Yb (**6b**)], and $[Eu(NCS)_2(thf)_4]_2$ (**7**) have been prepared in good to high yield by redox transmetallation between rare earth metals and the commercially available $Hg(SCN)_2$. In addition $[Eu(NCS)_3(dme)_2(\mu\text{-}dme)_{0.5}]_2$ (**1c**) and $[Yb(NCS)_3(dme)_2]$ (**1f**) have been prepared by oxidation of *rac*-**4c** and $[Yb(NCS)_2(thf)_2]$, respectively, with $Hg(SCN)_2$ in dme. Crystallisation of **1e** from dme/diglyme (diglyme = bis(2-methoxyethyl) ether) and thf yields $[Er(NCS)_3(diglyme)(dme)]$ (**2**) and $[Er(NCS)_3(thf)_4]_2$ (**3g**), respectively, and prolonged storage of *rac*-**4a** in cold dme gave $[Ca(NCS)_2(dme)_2(H_2O)]$ (**5**). All undergo rapid hydrolysis on exposure to air. Two structural breaks are observed for $[RE(NCS)_3(dme)_n]$ complexes, all of which have solely RE–NCS binding. Compounds **1a**,**b** are nine-coordinate monomers that differ in the arrangement (T or Y) of the $RE(NCS)_3$ moiety, **1c**–**e** are eight coordinate dinuclear complexes being bridged by a single $\eta^1{:}\eta^1$-(*O*,*O*′)-dme and **1f** is a seven coordinate monomer. **2** is an eight coordinate monomer with, unusually for the present complexes, a facial $RE(NCS)_3$ array. By contrast **3a**–**g** are all dimeric, eight coordinate complexes with two unusual RE–NCS–RE bridges. The RE–S bonds are very weak and show little variation with RE^{3+} radius, and Er–S of **3g** increases by 0.18 Å between 123 K and room temperature), foreshadowing a change to a seven coordinate monomer with $[Yb(NCS)_3(thf)_4]$. Monomeric eight coordination with *transoid* (N–RE–N ≈ 149°) SCN–RE–NCS bonding is observed in *rac*-**4a**–**c** and Λ-**4c**, whilst **5** is a seven-coordinate monomer with a *cis*-$Ca(NCS)_2$ array. Single crystals of **6**,**a**,**b** contain seven-coordinate, pentagonal bipyramidal monomers with *trans*-NCS ligands, whereas **7** is dimeric with two Eu–NCS–Eu bridging ligands and seven coordination for Eu.

Introduction

Anhydrous rare earth halides, REX_3 (X = Cl, Br, I) are commonly used reagents for the synthesis of rare earth organometallics (particularly cyclopentadienyls), alkoxides, aryloxides and organoamides.[1] For many laboratory syntheses, tetrahydrofuran (thf) or 1,2-dimethoxyethane (dme) solvated rare earth halide derivatives are attractive alternative reagents having higher solubility and a variety of convenient synthetic routes.[2] Solvated lanthanoid halides have a rich structural chemistry, particularly for the $[REX_3(S)_x]$ (X = Cl, Br, I; S = thf, dme; x = 1–5) complexes, which include the charge separated X = Cl, x = 3.5 species, with the lanthanoid contraction having a major effect.[2] Less is known of the structures of the analogous rare earth pseudohalide thiocyanate complexes, though a number of complexes of the form $[RE(NCS)_3(L)_n]$ have been reported with both monodentate[3] and polydentate[4–9] coligands completing the coordination sphere. Of particular interest, are the dimeric lanthanoid thiocyanate species $[RE(NCS)_3(thf)_4]_2$ (RE = Nd, Sm, Eu, Gd, Tb, Dy, Ho, Er) prepared by the metathesis route between $RECl_3$ derivatives and three equivalents of KSCN in thf.[10,11] This series shows an unusual binding mode {which has been observed once since in divalent $[Eu(NCS)_2]_\infty$}[12] where one thiocyanate ligand bridges between two RE metal centres through the N donor atom and, surprisingly for a hard metal, the S donor atom. A structural change is observed late in the lanthanoid series since the Yb derivative is a seven-coordinate monomer, $[Yb(NCS)_3(thf)_4]$.[13,14] The only trivalent example of a dme-coordinated rare earth thiocyanate complex is the separated ion pair $[Ph_3PNH_2(OEt_2)][Sm(NCS)_4(dme)_2]$.[15] Thiocyanatolanthanoidate(III) complex anions have been recently found in the ionic liquids $[Cat_{5-x}][Ln(NCS)_{8-x}(H_2O)_x]$ (x = 0–2; Cat = 1-butyl-3-methylimidazolium or 1-hexyl-3-methylimidazolium),[16] and earlier in $[NMe_4]_3[RE(NCS)_6(H_2O)]$ (RE = La – Er) and $[NMe_4]_4[RE(NCS)_7]$ (RE = Dy, Er, Yb).[17] There are three related di-

[a] School of Chemistry, Monash University, Clayton, Vic. 3800, Australia
Fax: +61-3-99054597
E-mail: glen.deacon@sci.monash.edu.au
peter.junk@sci.monash.edu.au

Supporting information for this article is available on the WWW under http://dx.doi.org/10.1002/ejic.201000111.

valent rare earth thiocyanate species namely $[Yb(NCS)_2(dme)_3]$[14] the unsolvated polymeric $[Eu(NCS)_2]_\infty$[12] and "$[Yb(NCS)_2(thf)_2]$", the last not yet crystallographically characterised as it is obtained as a powder due to lability of coordinated thf in initially isolated single crystals.[14]

We now report a structural study of $[RE(NCS)_3(dme)_x]$ (x = 2, 2.5, 3) complexes prepared utilising redox transmetallation between RE elements and the commercially available mercuric thiocyanate. The synthetic method, which has a simple work up procedure, has also been applied to the $[RE(NCS)_3(thf)_4]_2$ complex series and the structural characterisation has been extended to RE = Y, La, Dy, Ho, and the RE = Er structure has been determined at low temperature revealing a surprising difference from the room temperature structure.[11] We also report analogous preparations and structure determinations of divalent lanthanoid and Ca thiocyanate complexes with dme, MeCN and thf coligands. The resulting two structurally well defined series of both trivalent and divalent rare earth thiocyanate complexes may be considered as possible reagents for salt elimination reactions in cases where halide and/or alkali metal retention is a problem.

Results and Discussion

Syntheses

The complexes $[RE(NCS)_3(dme)_n]_b$ [RE = La (**1a**), Nd (**1b**), n = 3, b = 1; Dy (**1d**), Er (**1e**), n = 2.5, b = 2] and $[RE(NCS)_3(thf)_4]_2$ [RE = Y (**3a**), La (**3b**), Nd (**3c**), Sm (**3d**), Dy (**3e**) or Ho (**3f**)] have been synthesised by redox transmetallation reactions between an excess of rare earth metal and dried $Hg(SCN)_2$ in dme or thf [Equation (1)]. $[Er(NCS)_3(diglyme)(dme)]$, (**2**), was crystallised from a mixed dme/diglyme solvent system [Equation (2)]. Complexes $[M(NCS)_2(dme)_3]$ {M = Ca *rac*-**4a**, Sm *rac*-**4b**, Eu *rac*-**4c** [Λ-**4c** was identified in crystals obtained at room temperature, and *rac*-**4c** crystallized at 5 °C]}, $[M(NCS)_2(NCMe)_5]\cdot NCMe$ [M = Ca (**6a**), Yb (**6b**)] and $[Eu(NCS)_2(thf)_4]_2$ (**7**) were also synthesised by redox transmetallation reactions [Equation (3)] with a larger excess of metal powders in dme, acetonitrile or thf. Complexes $[Eu(NCS)_3(dme)_{2.5}]_2$ (**1c**) and $[Yb(NCS)_3(dme)_2]$ (**1f**) were synthesised by oxidation of *rac*-**4c** or $[Yb(NCS)_2(thf)_2]$[14], respectively, with $Hg(SCN)_2$ in dme [Equation (4)]. $[Ca(NCS)_2(dme)_2(H_2O)]$ (**5**), was isolated as a minor product from one reaction attempting to synthesise *rac*-**4a**.

The reaction mixtures for **1**, **3**, **4**, **6**, **7** were stirred at ambient temperature and/or sonicated. The initial appearance of precipitated mercury was often observed within 1 d but the reactions were allowed to continue for an extended time to ensure higher yields. In the case of **3a**–**3f**, this method was more effective than use of activation with Hg metal or I_2 or heating. The yields of compounds **1a**–**f** by reactions (1) and (4), of **3a**–**3f** by reaction (1) and of divalent complexes by reaction (3) were good to high (50–99%). Crystallization of **1a**–**f** requires quite precise conditions (see Exp. Sect.) and high yields of **3a**–**f** requires several

$$2\ RE^0 + 3\ Hg(SCN)_2 \xrightarrow{solv} a\ [RE(NCS)_3(solv)_n]_b + 3\ Hg\downarrow$$

RE = La (**1a**), Nd (**1b**)
solv = dme; n = 3; a = 2, b = 1

RE = Dy (**1d**), Er (**1e**)
solv = dme; n = 2.5; a = 1; b =2

RE = Y (**3a**), La (**3b**), Nd (**3c**), Sm (**3d**), Dy (**3e**), Ho (**3f**)
solv = thf; n = 4; a = 1; b = 2 (1)

$$[Er(NCS)_3(dme)_{2.5}]_2 \xrightarrow[diglyme]{dme} 2\ [Er(NCS)_3(diglyme)(dme)] \quad (2)$$

$$M^0 + Hg(SCN)_2 \xrightarrow{solv} [M(NCS)_2(solv)_x]_y\cdot z\ solv + Hg\downarrow$$

M = Ca *rac*-(**4a**), Sm *rac*-(**4b**), Eu *rac*-(**4c**) Λ-(**4c**)
solv = dme; x = 3; y = 1; z = 0

M = Ca (**6a**), Yb (**6b**)
solv = MeCN; x = 5; y = 1; z = 1

M = Eu (**7**)
solv = thf; x = 4; y = 2; z = 0 (3)

$$2\ [RE(NCS)_2(solv)_n] + Hg(SCN)_2 \xrightarrow{dme} 2\ [RE(NCS)_3(dme)_x]_y + Hg\downarrow$$

RE = Eu; solv = dme; n =3
RE = Yb; solv = thf; n = 2

RE = Eu (**1c**); x = 2.5; y = 2
RE = Yb (**1f**); x = 2; y = 1 (4)

extractions of the metallic residues with thf. In general, freshly filed metal gave higher yields than commercial filings. By comparison, the metathesis method used by Depaoli et al. for $[RE(NCS)_3(thf)_4]_2$ complexes involved centrifugation to remove precipitated KCl and yields for this method were not reported.[11] Earlier preparations by this method (without structural characterisation) gave yields of 29–71% with samples containing 1–3% KCl and, for Ln = Ho, Er, Yb, 1.5–4.4% KSCN.[10] This alkali metal and/or chloride retention illustrates one of the disadvantages of the metathesis route and points to the value of the current syntheses [see Equations (1), (3), (4)], which give higher yields.

Although the metal, and/or SCN^- and/or elemental (C, H, N) analyses of the bulk samples generally matched

the compositions indicated by the crystal structures, there were three exceptions. Whilst a metal analysis on freshly isolated crystals of **3b** corresponded to $[La(NCS)_3(thf)_4]_2$, a powder sample analysed as $La(NCS)_3(thf)_{3.25}$. A similar composition was indicated by microanalysis of a crystalline sample after storage. Complexes **6a**,**b** also gave elemental analyses indicating compositions different from their crystal structures. Analysis of **6a** indicated the composition $[Ca(NCS)_2(NCMe)_2]$ compared with the $[Ca(NCS)_2(NCMe)_5]$·MeCN composition of the crystals. The lability of coordinated acetonitrile molecules in group 2 complexes has been noted previously for complexes $[MI_2(NCMe)_5]$ (M = Ca, Sr).[18] Solutions of **6b** were deep red in colour as was the oily solid remaining after the solvent was removed under reduced pressure. Further drying of **6b** by heating caused the red oily solid to become a yellow/brown powder. The red solid and yellow/brown powder have different levels of solvation (2.5 and 0.6 MeCN/Yb, respectively) much less than in fresh crystals $\{[Yb(NCS)_2(NCMe)_5]$·MeCN$\}$. All complexes are very sensitive to atmospheric moisture, and are rapidly decomposed on exposure to air.

The solubilities given in the Exp. Section (0.6–1.2%, w/v) are in situ values from the amount of compound isolated from a measured volume of solution after the preparation. They may be greater than on redissolving isolated products. Generation in situ may be the best approach if the compounds are to be used for further reactions. Redox-transmetallation is eminently suited for this purpose.

X-ray Crystallography

Because of the large number of structures, all tables of bond lengths and angles are given as Supporting Information.

a) Trivalent dme Complexes

The structural changes that occur with change of lanthanoid are displayed in Figure 1.

Compounds **1a** and **1b** are monomeric complexes containing nine-coordinate metal centres comprising three RE–N bonds and six RE–O bonds (Figure 1, a). The thiocyanate ligands are *N*-bound to the rare earth metal centre. Each of the three dme molecules chelates to the metal centre in an unsymmetrical fashion through the two oxygen donor atoms. Considering the geometry of the thiocyanate ligands only, complex **1a** exhibits a distorted T-shape geometry with a *mer* configuration and one *transoid* N–La–N angle. In contrast, the geometry displayed in **1b** by the thiocyanate ligands is distorted trigonal planar (Y-shaped) with two *transoid* N–Nd–N angles (Table S1). There are reported examples of both distorted T[3,4,13,14,19] and distorted trigonal planar[7–9,11,20] $Ln(NCS)_3$ geometry.

Compound **1a** crystallises in the space group $P2_1/c$. The asymmetric unit is comprised of two isolated monomers which show the same connectivity but differ slightly from each other in bond lengths and angles (Table S1). The La(1) monomer is a distorted tricapped trigonal prism while the geometry of the La(2) monomer is best described as a distorted capped square antiprism.[21,22] The average La–N and La–O bond lengths for La(1) and La(2) are 2.53 and 2.64 Å and 2.52 and 2.66 Å respectively. These values compare well with the range of La–NCS [2.548(4)–2.577(4) Å] and La–O [2.578(3)–2.645(3) Å] bond lengths displayed by nine-coordinate $[La(NCS)_3$(dibenzyldiaza-18-crown-6)$]$.[5] The La–N bond lengths in **1a** are similar to the corresponding terminal bond lengths in eight-coordinate $[La(NCS)_3(thf)_4]_2$ (**3b**) (below) despite the 0.06 Å difference between the ionic radii of eight- (1.160 Å) and nine- (1.216 Å)[23] co-

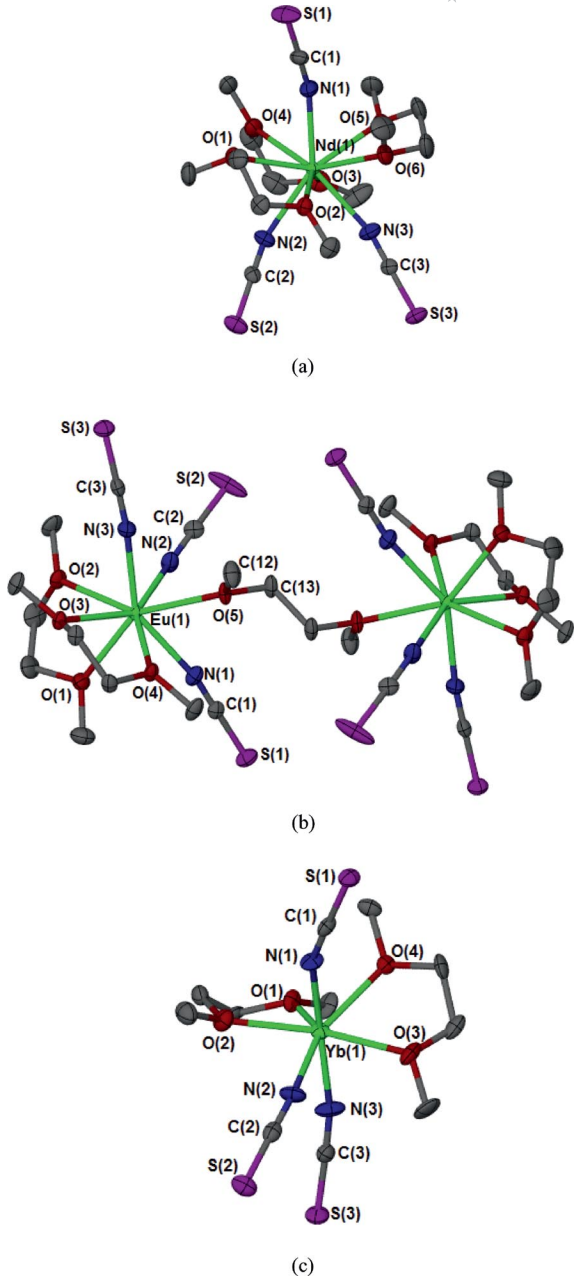

Figure 1. a) Monomeric structure of $[Nd(NCS)_3(dme)_3]$ (**1b**). Compound **1a** has a similar structure; b) dinuclear structure of $[Eu(NCS)_3(dme)_2(\mu\text{-}dme)_{0.5}]_2$ (**1c**). Compounds **1d** and **1e** are isotypic; c) monomeric structure of $[Yb(NCS)_3(dme)_2]$ (**1f**). Ellipsoids shown at 50% probability and hydrogen atoms omitted for clarity.

ordinate lanthanum cations. Conversely, the difference between the average La–O bonds in **1a** and **3b** is somewhat larger than expected (0.08 Å).[23]

Compound **1b** crystallises in the space group $P2_1/n$ where the asymmetric unit consists of a nine-coordinate monomer with distorted tricapped trigonal prismatic stereochemistry similar to the La(1) monomer in **1a**. The three Nd–N bond lengths in **1b** (Table S1) are very similar to each other with an average length of 2.47 Å. This is equivalent to the average La–N bond length in **1a** (2.53 Å) allowing for the decrease in ionic radii between La^{3+} and Nd^{3+} (0.058 Å).[23] However, the average terminal Nd–N bond length also agrees with that of 2.47 Å in eight-coordinate $[Nd(NCS)_3(thf)_4]_2$[11] (**3c**) despite the change in coordination number. Furthermore, the average Nd–N bond length in **1b** is comparable to the Nd–NCS bond lengths in $[Nd(NCS)_3$(dibenzyldiaza-18-crown-6)] [2.449(3)–2.522(2) Å][24] but shorter than those reported in $[Nd_2(\mu\text{-}OAc)_2(NCS)_4(C_5H_5NO)_2(H_2O)_6]$ [2.511(5) and 2.540(4) Å].[25] The average Nd–O distance is shorter than <La–O> by close to the expected from ionic radii differences[23] and larger than <Nd–O> of eight-coordinate $[Nd(NCS)_3(thf)_4]_2$ also by the ionic radius difference.[23] The similarity between Ln–N bond lengths of nine-coordinate **1a**,**b** and eight-coordinate **3b**,**c**, respectively, may arise because of great crowding in the latter (Σ steric coordination numbers 8.04 and 8.44).[26]

The analytical data for **1c**–**e** suggest a $RE(NCS)_3(dme)_{2.5}$ composition and this is reflected in a structural change from **1a**,**b**. The coordination number of the rare earth metal centre decreases from nine to eight. Trivalent eight-coordinate Eu (1.120 Å) has an ionic radius 0.043 Å smaller than the corresponding Nd^{3+} radius (1.163 Å).[23] This lanthanoid contraction is enough to cause overcrowding at the metal centre and force one dme molecule to bind in a bridging rather than a chelating coordination mode. The sum of the steric coordination numbers (CN_S) of the ligands[26] decreases from 8.04 in **1a**–**b** to ca. 7.5 in **1c**–**e**.

Compounds **1c**–**e** are isotypic dinuclear complexes (Figure 1, b), crystallising in the monoclinic space group $P2_1/n$ where the asymmetric unit comprises half of the molecular unit. The metal centres are coordinated to three *N*-bound thiocyanate ligands and five oxygen donor atoms from two chelating and one bridging dme ligands where the geometry about the metal centre can be described as a distorted square antiprism (see Supporting Information, Figure S1).[22,27] [N(3), O(5), O(3), O(4)] are in one distorted square plane while N(2), N(1), O(2), O(1) are in the second. The chelating dme molecules are *cisoid* to each other.

The RE–N and RE–O bond lengths shorten as the atomic number increases due to lanthanoid contraction (see Supporting Information, Table S2). The average RE–N bond lengths are Eu = 2.40; Dy = 2.35; Er = 2.34 Å. The Eu–N bond lengths in **1c** are similar to or slightly shorter than observed in the eight-coordinate Eu^{3+}/Ni^{2+} bimetallic structure $[Eu_2Ni(NCO)_8(dmf)_8]$ (dmf = *N*,*N*-dimethylformamide) [$Eu–N_{(terminal)}$ = 2.422(6) Å][28] and similar to the average terminal thiocyanate Eu–N bonds in eight-coordinate $[Eu(NCS)_3(thf)_4]_2$.[11] The Dy–N bond lengths in **1d** fall in the middle of the range displayed in the eight-coordinate complex $[Dy(NCS)_3$(dibenzo-30-crown-10)$(H_2O)_2]\cdot H_2O\cdot$MeCN [2.26(2)–2.402(9) Å][29] and are similar to the average terminal Dy–N bond length in complex **3e** (below). Eight-coordinate complexes $[Er(NCS)_3$(1,8-naphtho-16-crown-5)][30] and $[Er_2(NCS)_3\{(py)_2C(OMe)O\}_3(MeOH)]\cdot$MeOH[31] (py = 2-pyridyl) report average Er–N bond lengths of 2.32 and 2.36 Å, respectively, which flank the corresponding lengths in **1e** whilst the terminal thiocyanate Er–N bonds in **3g** (ave. 2.33 Å) are comparable.[11] The N–RE–N angles in complexes **1c**–**e** (Table S2) indicate distorted T-shaped geometry for $Ln(NCS)_3$ similar to that of **1a**.

The average RE–O bond lengths in **1c**–**e** (Eu = 2.48; Dy = 2.45; Er = 2.43 Å) decrease in accordance with the lanthanoid contraction, and are comparable with those of $[Eu(NCS)_3(thf)_4]_2$,[11] **1d** and **1e**, respectively.

Various rare earth structures containing an unidentate dme are known,[32–35] whilst three reported rare earth metal complexes possess a bridging dme molecule namely; $[Nd_2(OCH\text{-}iPr_2)_6(\mu\text{-dme})]_\infty$,[36] $[Nd(tBu_2pz)_3(\mu\text{-dme})]_\infty$ (tBu_2pz = 3,5-di-*tert*-butylpyrazolate)[37] and $[\{YbI_2(dme)_2\}_2(\mu\text{-dme})]$.[38] The last is the most similar to **1c**–**e** as it features bridging bidentate and chelating dme molecules and has a dinuclear structure. Seemingly, the chelating dme molecules prevent further aggregation.

A further structural change was observed between Er and Yb as **1f** was found to be a seven-coordinate monomer which crystallises in the $P2_1/c$ space group (Figure 1, c). The very small decrease in ionic radii between Er^{3+} and Yb^{3+} (0.019 Å)[23] causes enough increased steric crowding to eliminate the bridging dme of **1c**–**e**. The stereochemistry is distorted pentagonal bipyramidal where the pentagonal plane contains atoms N(2) O(3), O(1), O(4), O(2) and the axial positions N(1) and N(3) [N(1)–Yb–N(3) 170.6(3)°].

The average Yb–N bond length is 2.29 Å (Table S3) which is shorter than Er–N bonds in **1e** (2.34 Å) and the difference is related to the lanthanoid contraction and the decrease in coordination number.[23] The average Yb–N bond lengths in the trivalent seven-coordinate monomer $[Yb(NCS)_3(thf)_4]$ (2.27 Å)[13] are comparable with **1f**. The thiocyanate ligands with N–Yb–N angles 170.6(3), 89.0(3) and 82.4(4)° form a distorted T-shaped array similar to those of **1a**,**c**–**e**. The average Yb–O bond length is 2.35 Å which is appropriately shorter than the average Er–O bond length in **1e** (2.43 Å).

b) Complex 2

The monomeric mixed solvent complex, **2**, crystallises in the $P2_1/n$ space group with an eight-coordinate Er atom bonded to three *N*-bound thiocyanate ligands and five oxygen donor atoms (three from the diglyme moiety and two from dme) (Figure S2). The donor atoms are positioned about the metal centre in a distorted bicapped trigonal prismatic array (Figure S2) and the thiocyanate ligands are in a facial arrangement (see Table S4 for N–Er–N angles), in contrast to Y and T arrangements in **1a**–**f**. The extra chelat-

ing arm of the diglyme molecule forces the thiocyanate ligands to position on one side of the Er cation face in a 3-legged stool geometry (Figure S2). Other complexes displaying a similar $Ln(NCS)_3$ array include $[Er(NCS)_3$(naphtho-16-crown-5)][30] where the arrangement is forced by the multidentate co-ligand.

Complex **2** displays comparable bond lengths (Table S4) to the eight-coordinate **1e** (Table S2). Thus, the average Er–N bond length in **2** is 2.32 Å (2.34 Å, **1e**).

The monomeric units of **2** are packed in columns one below the other in the corners and centre of the unit cell when viewed down the *c*-axis (Figure S3).

c) Trivalent thf Complexes

Initially, the structures of $[RE(NCS)_3(thf)_4]_2$ [RE = Y (**3a**), La (**3b**)] were determined (at 123 K) to extend the reported room temperature structures[11] of RE = Nd (**3c**), Eu and Er (**3g**) to the group 3 elements. Unexpectedly, a 0.18 Å difference between the Y–S bond length and the previously determined Er–S value was observed, far more than expected from the difference in measurement temperatures and the 0.015 Å difference in ionic radii between Y^{3+} and Er^{3+}.[23] Consequently, we have further extended the structure determinations to elements of similar size, viz. RE = Dy (**3e**) and Ho (**3f**) as well as examining the structure of **3g** at 123 K.

All structures **3a**, **3b**, **3e**–**g** were found to be dimeric with the unusual (for hard metals) RE–NCS–RE bridging and eight-coordination of the metal atoms (Figure S4) as reported for RE = Nd, Eu, Er[11] on the basis of room temperature studies. The bridging is illustrated for the new divalent complex $[Eu(NCS)_2(thf)_4]_2$ (**7**) (Figure 3 below). In particular, there is no structural change with the larger RE ions−La, (**3b**), Nd (**3c**)−in contrast to $[Ln(NCS)_3(dme)_n]$ where there is a change between RE = Nd (**1b**) and Eu (**1c**). The distorted antiprismatic stereochemistry has a Y-shape arrangement of the three RE–N bonds, with a terminal and a bridging nitrogen enclosing the narrow N–RE–N angle (Table S5). By contrast, the three S–RE–N angles exhibit a distorted T shape at RE. The RE–N bond lengths in the current determinations decrease by 0.19 Å from **3a** to **3g**, somewhat more than the 0.16 Å expected from the lanthanoid contraction,[23] whereas the shortening of RE–O corresponds to that expected (Table S5). As already indicated above, the terminal RE–N and the RE–O bond lengths are similar to those of related dme complexes **1a**–**e**, and the bridging RE–N distance is only ca. 0.04–0.05 Å longer than terminal RE–N. On the other hand, the RE–S distance shows little change from **3b** to **3g**, **3a** (0.02–0.04 Å), but with a slight *increase* from **3e**,**f** to **3a**, **g** in defiance of the ionic radius decrease in the same sequence.

Bond lengths for **3c** and $[Eu(NCS)_3(thf)_4]$ at room temperature generally fit within the current data. However, the RE–S bond lengths of **3a**,**e**–**g** at 123 K are notably (0.18–0.20 Å) shorter than Er–S of **3g** at room temperature. Contrastingly, most Er–N(O) distances at 123 K and room temperature (Table S5) agree close to 3 e.s.d. values apart from a 0.05 Å difference in Er–O(3). Thus, the behaviour of the Er–S bond length is remarkable and unique. A redetermination of the unit cell of **3g** at room temperature was in satisfactory agreement with that reported[11] transformed from $P2_1/a$ to $P2_1/c$ of the present structure, and unit cells of **3c**,**d** also agree with those reported.[11] Transformation of the larger (ca. 100 $Å^3$) room temperature unit cell to $P2_1/c$ and refinement with the low temperature data gave a larger Er–S value of 3.19(1) Å but still below the 3.283(4) Å of the room temperature determination.[11]

All RE–S bond lengths are very long. Thus, La–S of eight-coordinate **3b** [3.121(2) Å] approaches La–S(thioether) [3.191(2), 3.237(2) Å] of *eleven*-coordinate $[La(\eta^5\text{-}C_5H_4CH_2CH_2SEt)_3]$,[39a] whilst Y–S of (**3a**) [3.1051(7) Å] is much longer than Y–S(thioether) [2.9572(6), 2.9379(6) Å] of nine-coordinate $[Y(\eta^5\text{-}C_5H_4CH_2CH_2SEt)_2Cl]$,[39b] indicating the S donor atoms of **3a**,**b** are behaving as neutral donors (S = C=N$^-$). By contrast, $C_6F_5S^-$ in $[Er(SC_6F_5)_3(dme)_2]$ has Er–S [2.694(2)–2.722(1) Å],[39c] much shorter than in **3g**.

On warming from 123 K to room temperature, the structure expands mainly by lengthening the Er–S bonds within the dimeric array (Figure S4). This, together with the unusual behaviour of the RE–S bond lengths with decrease in the ionic radius at low temperatures foreshadow the structural change to the seven-coordinate monomer[13,14] $[Yb(NCS)_3(thf)_4]$. Subtraction of the RE^{3+} ionic radius from bond lengths (Table S5) gives a narrow range 1.33–1.37 Å from RE–N values, the larger value associated with the bridging RE–N bond, but a much wider range 1.33–1.52 Å from RE–O data. These are still within the large range of values derived from RE–O(ether) bond lengths.[40] The larger values 1.42–1.52 Å are for RE–O(3,4) where the oxygen atoms are *transoid* to bridging thiocyanate N or S donors. Nevertheless a large *trans* influence of the latter seems unlikely, given the weak RE–S interaction and the lengthening may be associated with steric repulsion between *cis* thf ligands.

d) Divalent dme Complexes

Complexes *rac*-**4a**–**c** and $[Yb(NCS)_2(dme)_3]$[14] are isotypic eight-coordinate monomeric species (Figure 2, a) where the asymmetric unit consists of half of the monomer and the equivalent atoms are generated by the twofold rotation axis (–*x*, *y*, –*z* + 3/2). The metal centre displays distorted dodecahedral geometry[22] (Figure S5) and is ligated by two *transoid N*-bound thiocyanate ligands and six oxygen donor atoms from three bidentate dme molecules. A single crystal of Λ-(**4c**) was also isolated and the structure determined (Figure 2, b). There is a complete molecule in the asymmetric unit.

There is a precedent for the isolation of separate configurational isomers of eight-coordinate divalent lanthanoid dme complexes, since $[SmI_2(dme)_3]$ forms crystals with different unit cell parameters depending on the crystallisation conditions.[41] At lower temperatures, the single crystals contain a racemic mixture of left hand (Λ) and right hand

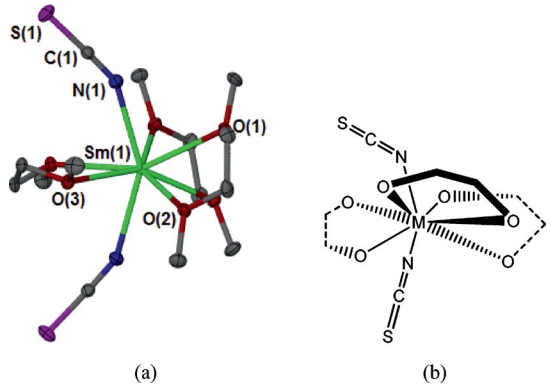

Figure 2. (a): The molecular structure of complex *rac*-**4b**. Compounds *rac*-**4a**,**c** are isotypic. Hydrogen atoms are omitted for clarity and the ellipsoids are shown at 50% probability; (b): schematic representation of the Λ-enantiomer, Λ-**4c**. Methyl groups omitted for clarity.

(Δ) screw stereoisomers. At room temperature, the crystalline product is a mixture of enantiomerically pure (Λ or Δ) single crystals.[41] In the present case, only Λ-**4c** was identified in the crystals obtained at room temperature (though Δ crystals must also be present), and then *rac*-**4c** crystallized at 5 °C. The unit cell dimensions of Λ-**4c** (see Exp. Section) are similar to those of Λ-[$SmI_2(dme)_3$].[41]

Only one of the M–N (M = Ca, Sm, Eu) bond lengths (Table S6) is unique in complexes *rac*-**4a**–**c** and the lengths vary according to the eight-coordinate divalent metal ionic radii (Ca 1.12, Eu 1.25, Sm 1.27 Å)[23] with Ca–N 2.448(2), Eu–N 2.598(2) and Sm–N 2.604(2) Å. The Yb–N bond length reported in [$Yb(NCS)_2(dme)_3$] (2.481(2) Å][14] is somewhat longer than observed for *rac*-**4a** although the ionic radii of Ca^{2+} and Yb^{2+} differ only by 0.02 Å.[23]

Eight-coordinate Ca^{2+} structures related to *rac*-**4a** include [$Ca(NCS)_2(H_2O)$(tetraglyme)] (tetraglyme = 2,5,8,11,14-pentaoxapentadecane) [Ca–N 2.444(4) (comparable), 2.488(4) Å (similar to Yb–N)][42] and [$Ca(NCS)_2$L] {L = 1,2-bis[2-(*o*-hydroxyphenoxy)ethoxy]ethane} [Ca–N 2.446(2), 2.427(2) Å].[43] *rac*-**4b** appears to be the only example of a divalent eight-coordinate thiocyanatosamarium complex. In eight-coordinate [$Sm(Ph_2pz)_2(dme)_2$] (Ph_2pz = 3,5-diphenylpyrazolate) the Sm–N bond lengths [2.556(3), 2.538(3) Å][44] are shorter than in *rac*-**4b** despite the use of a bulkier ligand and delocalization of the negative charge across two nitrogen donor atoms.

A wide range of M–O (M = Ca, Sm, Eu) bond lengths can be observed within each solid-state structure (Table S6) where M–O(2) is consistently the shortest. Eight-coordinate [$Ca(Ph_2pz)_2(thf)_4$] [2.494(2)–2.502(2) Å],[45] and [Ca{(*p*-MeC_6H_4)NNN-(*p*-MeC_6H_4)}$_2$(dme)$_2$] [2.488(2) and 2.561(2) Å][46] display Ca–O bond lengths within the range observed in *rac*-**4a**. Eight-coordinate *rac*-[$SmI_2(dme)_3$] displays longer Sm–O bond lengths [2.652(10)–2.746(9) Å][41] than *rac*-**4b** perhaps owing to the greater steric demands of iodide than NCS^-.[26] Eight-coordinate divalent [$EuI_2(dme)_3$] has an average Eu–O bond length of 2.66 Å[47] which is at the upper end of the range for *rac*-**4c**.

The Eu–N and Eu–O bond lengths and N–Eu–N angles in *rac*-**4c** and Λ-**4c** (Table S6) are all comparable, but the Eu–N–C bond angles differ somewhat [153.1(2) and 159.4(2)/155.0(3)° respectively].

The *transoid* N(1)–M–N(1)# angles in *rac*-**4a**–**c** and Λ-**4c** are 148.60(7), 149.59(9), 149.4(1) and 149.41(8)° respectively, less linear than the I–RE–I angle of Λ-[$SmI_2(dme)_3$] [158.18(2)°][41] and *rac*-[$SmI_2(dme)_3$] [180 and 157.65(2)°][41,48] [see also 157.94(2) and 178.45(2)°][49] and I–Eu–I of [$EuI_2(dme)_3$] (158.51°).[47] The sum of the ligand steric coordination numbers are larger in [$REI_2(dme)_3$] (8.3)[26] than in [$RE(NCS)_2(dme)_3$] (8.0)[26] though both are substantially crowded. Indeed, this is reflected in the formation of the less crowded [$Ca(NCS)_2(dme)_2(OH_2)$] (**5**) (Σ steric CN = 7.1) on storage of a dme solution of *rac*-**4a** at 5 °C for an extended period. **5** is a monomeric complex with a seven-coordinate Ca^{2+} metal centre bonding to two now *cis N*-bound thiocyanate ligands and five (two bidentate dme ligands and one water ligand) oxygen donor atoms (Figure S6). The geometry at the metal centre is described as distorted pentagonal bipyramidal[22] where the N(2) and O(1) atoms are in the axial positions and the atoms N(1), O(2), O(3), O(4) and O(5) form the pentagonal plane (Figure S6).

The Ca–N bond lengths in (**5**) (Table S7) are comparable with those of seven-coordinate [$Ca(NCS)_2$(triglyme)(H_2O)] (triglyme = 2,5,8,11-tetraoxadodecane) [2.389(5) and 2.397(5) Å].[50] In **5**, the Ca–OH_2 bond length [2.350(2) Å] is much shorter than the Ca–O(dme) bond lengths [2.4176(9)–2.5108(9) Å] which is also the trend exhibited in the solvent separated ion pairs [$Ca(H_2O)_3(dme)_2$][I]$_2$·dme [Ca–OH_2 2.348(3)–2.351(3), Ca–$O_{(dme)}$ 2.427(2)–2.471(3) Å][51] and [$CaBr(H_2O)_2(dme)_2$][Br] [Ca–OH_2 2.355(4)–2.372(4) Å, Ca–O(dme) 2.429(3)–2.487(4) Å];[52] *cisoid* N–Ca–N bond angles have also been observed in the analogous [$Ca(NCS)_2(H_2O)(bipy)_2$] [85.0(2)°][53] and [$Ca(NCS)_2$(triglyme)(H_2O)] [90.6(7)°].[50]

e) Divalent Acetonitrile Complexes

Compounds **6a**,**b** are isostructural monomeric complexes where the seven-coordinate metal centres form bonds to two *N*-bound thiocyanate ligands and five bonds to *N*-bound acetonitrile solvent molecules (Figure S7). Half of the monomeric unit is unique and included in the asymmetric unit (the ligand N(4)–C(6)–C(7)H_3, the lattice NCMe and the metal centre all are on special positions), the other half is generated by the twofold rotation axis (–*x* + 1, *y*, –*z* + 3/2). The geometry about the metal centres is distorted pentagonal bipyramidal (Figure S7b) which is not uncommon for group 2 and divalent lanthanoid diiodide derivatives[18,54] and the two thiocyanate ligands are *trans* to each other (cf. **5**) and the acetonitrile ligands are in the pentagonal plane.

The Ca–NCS bond in **6a** is 2.384(2) Å (Table S8) and Yb–NCS in **6b** 2.415(3) Å, the difference corresponding to the difference in ionic radii between seven-coordinate Ca^{2+} (1.06 Å) and Yb^{2+} (1.08 Å).[23] Seven-coordinate [$Ca(NCS)_2$-

$(H_2O)(bipy)_2$] has a longer average Ca–NCS bond length of 2.44 Å,[53] though it is less crowded.[26] A comparable length [2.481(2) Å] exists in eight-coordinate $[Yb(NCS)_2(dme)_3]$[14] after allowing for the change in coordination number.

The M–NCMe bond lengths in **6a** and **6b** (Table S8) are comparable, 2.549(2)–2.579(2) Å (Ca) and 2.565(3)–2.583(3) Å (Yb). The Ca–NCMe bond lengths are also comparable to those of the seven-coordinate $[CaI_2(NCMe)_5]$[18] [2.518(8)–2.566(8) Å].

Viewing the packing mode from the *b*-axis, the ligands form almost perfect boxes (Figure S8).

f) A Divalent thf Complex

$[Eu(NCS)_2(thf)_4]_2$ (**7**) is a dimeric structure where the asymmetric unit contains half of the dimer and the equivalent atoms are generated by inversion ($-x + 1, -y + 2, -z + 1$). Compound (**7**) displays the same unusual bridging coordination mode as **3a**–**g** where two thiocyanate ligands bridge between two identical metal centres through the N and S donor atoms (Figure 3). The polymeric divalent europium thiocyanate complex $[Eu(NCS)_2]_\infty$ also displays this unusual type of bonding.[12]

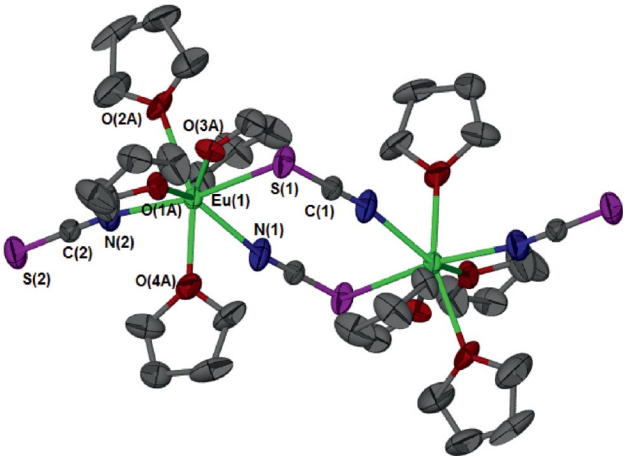

Figure 3. The dimeric structure of $[Eu(NCS)_2(thf)_4]_2$ (**7**). The ellipsoids are shown at 40% probability. The hydrogen atoms and the second part of the disordered thf molecules have been omitted for clarity.

The divalent Eu metal cations have a seven-coordinate environment with three thiocyanate ligands (two *N*-bound and one *S*-bound) and four thf molecules. The coordination geometry about the metal centre can be described as distorted pentagonal bipyramidal[22] (Figure S9).

The Eu–N bond lengths are 2.518(4) Å (terminal NCS) and 2.588(4) Å (bridging NCS – Table S9). These compare well with trivalent $[Eu(NCS)_3(thf)_4]_2$ [$Eu–N_{ter}$ (ave.) 2.40 Å and $Eu–N_{br}$ 2.450(5) Å][11] when the difference in the ionic radii of 0.13 Å between seven-coordinate Eu^{2+} and eight-coordinate Eu^{3+} [23] is considered. The terminal Eu–N bonds are significantly shorter than in seven-coordinate $[Eu\{N(PPh_2)_2\}_2(thf)_3]$[55] [2.565(3) and 2.603(3) Å] and near that of six-coordinate $[Eu\{N(SiMe_3)_2\}_2(dme)_2]$[56] [2.530(4) Å] where the anionic ligands are much bulkier.[26] In contrast to the very weak RE–S bonds of **3a**–**g**, the Eu–S bonding of **7** appears more significant. The Eu–S bond lengths (Table S9) are near those [3.014(3), 3.035(3) Å] of the eight-coordinate complex $[Eu(\mu\text{-}SC_6F_5)_2(thf)_2]_n$,[57] perhaps implying a contribution of $^-SC{\equiv}N$ character to the thiocyanate donor (unlike **3a**–**g**), and consistent with Eu^{II} softer than RE^{III}.

The large estimated standard deviations in the Eu–O bond lengths of **7** make comparisons with similar complexes less profitable. However, seven-coordinate divalent Eu complexes with comparable Eu–O bond lengths to <Eu–O> of **7** include $[Eu(t\text{Bu}_2\text{pz})_2(thf)]_2$ ($t\text{Bu}_2\text{pz}$ = 3,5-di-*tert*-butylpyrazolate, 2.583(1) Å],[58] $[EuI_2(thf)_5]$ (ave. 2.59 Å),[59] and $[Eu(C_6F_5)_2(thf)_5]$ (2.580(2)–2.647(2) Å].[60]

Infrared Spectroscopy

Although IR spectra have been extensively used in the elucidation of the nature of thiocyanate coordination[61–62] the extensive X-ray structure determinations of the present study have eliminated the need for IR in a primary role. Both monomeric **1a**,**b** show a single intense ν(CN) absorption in a region[61–62] for *N*-bonded thiocyanate complexes, though both *anti*-symmetric and symmetric modes are expected to be IR active.[61] However, dinuclear **1c**–**e** and mononuclear **1f** show some splitting of the intense absorption at 2058–2037 cm^{-1} (Experimental Section). A low intensity band at ca. 830 cm^{-1} corresponds to ν(CS) of N-bonded species.[61–62] Complex **2** with three *cisoid* N-ligated NCS ions has appropriate intense antisymmetric and symmetric ν(CN) absorptions and ν(CS) is observed at 830 cm^{-1}. Dinuclear RE–N–C–S–RE-bridged complexes **3a**–**g** show two intense absorptions, one near 2100 cm^{-1} and one near 2040 cm^{-1} attributable to antisymmetric and symmetric ν(CN) modes. Interestingly one appears in the region for M–S bonding and one in the region for M–N bonding. Likewise, ν(CS) absorptions are observed near 800 and 670 cm^{-1}, also corresponding to regions for *N* and *S* bonding respectively.[61–62] Complexes *rac*-**4a**–**c** show expected features for N-ligation and the N,S-bridged (**7**) has features similar to the similarly bonded trivalent **3a**–**g**. An additional weaker ν(CN) band at 2100 cm^{-1} in the spectrum of **4a** may derive from an N,S-bonded species formed by partial loss of dme on mulling or standing. All dme and thf complexes exhibited strong bands attributable to C–O stretching of the coordinated ethers at 1100–1000 cm^{-1} and 900–850 cm^{-1}, shifted from the free ligand values.[37,63] The spectra of **6a**,**b** are more problematic owing to loss of coordinated acetonitrile. Interestingly, the ν(CN) frequencies of the coordinated MeCN only lose intensity and do not change position as the ligand is lost on standing, even though structural changes would be expected.

Upon briefly exposing the Nujol mulls of **1a**–**f**, **2**, **3a**–**e**, *rac*-**4a**–**c**, **6a**,**b** and **7** to the atmosphere, all compounds decomposed. The ν(NC) band broadens and shifts to 2056–2090 cm^{-1} while δ(OH), appears between 1607–1635 cm^{-1} and a large broad band covers the ν(OH) region indicating H_2O/OH^- absorption.

Conclusions

Redox transmetallation between RE elements (or Ca) and mercuric thiocyanate in dme, thf and MeCN provides a high yield, simple route to a wide variety of solvent-coordinated trivalent and divalent rare earth thiocyanate complexes. This route avoids the problems of alkali metal halide or thiocyanate retention observed for the metathesis route.[10] Extensive structural characterisation of the resulting complexes has been made. Dme complexes $[RE(NCS)_3(dme)_n]$ (n = 2, 2.5, 3) form three main structural types: **1a**,**b** (RE = La, Nd; n = 3) are nine-coordinate monomers, which differ in the arrangement (T or Y) of the NCS groups; **1c**–**e** (RE = Eu, Dy, Er; n = 2.5) are dinuclear eight-coordinate complexes with a *single* μ-η^1:η^1-dme bridging the RE atoms, whilst (**1f**) (RE = Yb; n = 2) is a seven-coordinate monomer. By contrast $[REX_3(dme)_2]_n$ (X = Cl, Br; n = 1, 2) show only two structural types, a halide-bridged eight-coordinate dimer, and a seven-coordinate monomer.[2] Dme bridging is *not* observed. Low-temperature structure determinations of $[RE(NCS)_3(thf)_4]_2$ (**3a**, **3b**, **3e**–**g**) have extended previous room temperature structures showing an eight-coordinate dimeric RE–NCS–RE-bridged structure from RE = La (**3b**) to RE = Y (**3a**), Er (**3g**). Given that a single dme-bridged structure is preferred over NCS bridging in **1c**–**e**, S,N bridging appears a last resort when no other alternative is available. RE–S bond lengths are strikingly independent of RE ionic radius despite a contraction of 0.16 Å from La to Er, and for **1g** the Er–S bond length at room temperature is 0.18 Å longer than at 123 K though most other bonds are unaffected. The near structural consistency in the $RE(NCS)_3$/thf system (only a change with monomeric $[Yb(NCS)_3(thf)_4]$) contrasts the wide variety of structural types observed in the $RECl_3$/thf series (six different structures) and $REBr_3$/thf series (three structural types).[2] Divalent $[RE(NCS)_2(dme)_3]$ (RE = Sm, Eu) and $[Ca(NCS)_2(dme)_3]$ crystallize as eight-coordinate monomeric racemates, and Λ-$[Eu(NCS)_2(dme)_3]$ was also crystallized, whereas $[Ca(Yb)(NCS)_2(NCMe)_5]$ are seven-coordinate monomers. The divalent dme complexes are often structural analogues of the corresponding REI_2 complexes[41,47–49] contrasting the dissimilarities with halide complex structures seen for $RE(NCS)_3$ species. With $[Eu(NCS)_2(thf)_4]_2$, a seven-coordinate complex, RE–NCS–RE bridging also appears.

Experimental Section

General Considerations: All manipulations were carried out under an inert atmosphere of purified nitrogen using conventional glove box and Schlenk techniques due to the air and moisture sensitivity of the compounds. 1,2-Dimethoxyethane and tetrahydrofuran were distilled from sodium benzophenone ketyl over sodium wire, toluene and hexane were distilled from sodium wire and diglyme and acetonitrile were distilled from CaH_2 into dry storage flasks equipped with Teflon® taps and all were stored under nitrogen. $Hg(SCN)_2$ (Sigma Aldrich) was dried under vacuum and stored in the dry box. Commercial filings (Y, Nd, Sm) and metal ingots (Ca, La, Sm, Eu, Dy, Er and Yb) the latter being freshly filed before use, were from Rhône–Poulenc, Sigma Aldrich, Santoku or Tianjiao International and stored in the glove box under a nitrogen atmosphere. Freshly filed metal proved more reactive than commercial filings/powder. IR spectra were recorded between 4000–650 cm^{-1} as Nujol mulls between NaCl plates using a Perkin–Elmer 1600 FTIR instrument. Melting points were determined in sealed glass capillaries under nitrogen and are uncalibrated. Samples were sent in sealed glass pipettes under nitrogen to the Campbell Microanalytical Laboratory, Chemistry Department, University of Otago Dunedin, New Zealand for elemental analyses (C, H, N). Rare earth metal analyses were determined by titration of the undigested sample against a standardised Na_2H_2edta solution using Xylenol orange as the indicator and hexamine as the buffer. Thiocyanate analyses were determined by titration with 9.33×10^{-3} mol/L $Ag(NO_3)$ standard solution using ammonium iron(III) sulfate as the indicator.[10]

General Synthetic Protocol for Complexes 1a,b,d,e and 3a–f, *rac*-4a–c, 6a,b and 7: The metal powders/fresh filings in excess were combined with $Hg(SCN)_2$ (Table 1) in a Schlenk flask, which was then charged with 30–60 mL of dme for complexes **1a**,**b**,**d**,**e** *rac*-**4a**–**c**, 30–90 mL of thf for complexes **3a**–**f** and **7** or 35–50 mL of acetonitrile for complexes **6a**,**b** and the reaction mixture was stirred at ambient temperature and/or placed in a sonic bath until ca. 3 d after the appearance of the black mercury product. The mixture was allowed to stand at room temperature until the excess metal and mercury product had settled to the bottom of the reaction vessel. The supernatant solution was isolated by filtration through a filter cannula. For **1a**–**f** concentration to 2 mL often gave an oily solution. Heating the concentrated solutions led to precipitation of the product, which could only be redissolved by adding further dme. In the case of **3a**–**f**, maximum yield required several extractions of the solid residue with thf (50 mL). The filtrate was concentrated and single crystal formation was promoted by the methods detailed below. After the crystalline material was fully characterised the mother liquor was evaporated to dryness leading to the isolation of a greasy product for the trivalent dme series **1a**–**f** [washed with one aliquot of toluene (20 mL) to form a powder], a greasy product for the divalent dme species *rac*-**4a**–**c** (but after extended drying this formed a powder), a powder for both the trivalent and divalent thf species **3a**–**f** and **7** and an oily product with a honeycomb appearance upon heating with a heat gun for the acetonitrile derivatives **6a**,**b**. Yield and solubility calculations included powder and crystalline material as both gave comparable IR spectra, except for **6a**,**b** where the composition of the bulk sample determined by elemental analyses was used rather than the crystal structure formula. Further extractions of the initial excess metal/precipitated elemental mercury solids, with the appropriate hot solvent, were often required to increase the yield above 50%, especially in the case of **3a**–**f**.

dme Complexes of $RE(NCS)_3$

$[La(NCS)_3(dme)_3]$ (1a): The pale yellow filtrate was concentrated to 10 mL and deposited colourless rod-shaped single crystals upon storage at 5 °C; m.p. 268–272 °C. IR (Nujol): $\tilde{\nu}$ = 2041 (vs), 1295 (w), 1250 (w), 1189 (m), 1093 (s), 1045 (vs), 1020 (sh), 977 (m), 965 (sh), 854 (s), 822 (vw) cm^{-1}. $C_{15}H_{30}La_1N_3O_6S_3$ (583.52): calcd. La 23.80, NCS 28.87; found La 23.46, NCS 28.86.

$[Nd(NCS)_3(dme)_3]$ (1b): The blue filtrate was concentrated to 10 mL and deposited blue block-shaped crystals upon storage at 5 °C; m.p. 182–187 (dec. 301) °C. IR (Nujol): $\tilde{\nu}$ = 2038 (vs), 1298 (w), 1245 (w), 1187 (w), 1113 (w), 1087 (m), 1040 (vs), 1013 (m), 976 (w), 865 (sh), 853 (m), 668 (m) cm^{-1}. $C_{15}H_{30}N_3Nd_1O_6S_3$ (588.85): calcd. C 30.59, H 5.14, N 7.14; found C 30.28, H 5.11, N 7.24.

Table 1. Details for the syntheses of **1a**–**f**, **2**, **3a**–**e**, *rac*-**4a**–**c**, **5**, **6a**,**b**, **7**.

Product	RE [mmol]	$Hg(SCN)_2$ [mmol]	Solvent (vol/ml)	Time [d] stirring	ultrasound	Solubility of product g [mmol] per 100 mL	Yield [%][a]
1a La	6.3	3.1	dme (30)	3	0	0.9 (1.5)	87
1b Nd[b]	6.3	3.2	dme (40)	4	2	1.2 (2.0)	68
1c Eu	–	–	dme (30)	3	0	0.9 (1.6)	67
1d Dy	3.2	1.6	dme (30)	4	0	0.8 (1.4)	77
1e Er[b]	5.0	2.5	dme (35)	4	3	1.2 (2.2)	71
1f Yb	–	–	dme (30)	3	0	1.0 (1.9)	87
2 Er[b]	5.0	2.5	dme (35)	4	3	–	7
3a Y[b]	8.0	2.7	thf (60)	4	4	0.7 (1.2)	62
3b La	5.0	2.5	thf (90)	5	0	0.9 (1.5)	99
3c Nd[b]	6.3	3.2	thf (60)	0	7	0.5 (0.8)	80
3d Sm[b]	6.3	3.2	thf (60)	0	7	0.6 (1.0)	65
3e Dy	1.6	1.6	thf (30)	3	1	1.0 (1.6)	65
3f Ho	2.4	2.0	thf (20)	3(12)[c]	0		54
rac-**4a** Ca	7.5	1.6	dme (60)	6	0	1.0 (2.3)	79
rac-**4b** Sm	3.1	1.0	dme (25)	5	0	1.1 (2.0)	51
rac-**4c** Eu	2.5	1.0	dme (45)	5	0	0.8 (1.5)	52
5 Ca	–	–	dme (–)	–	–	–	7
6a Ca[d]	7.5	2.5	MeCN (50)	5	0	0.9 (3.8)	77
6b Yb[d]	5.0	2.5	MeCN (35)	5	0	1.0 (2.6)	69
7 Eu	9.3	2.5	thf (30)	5	0	0.9 (1.6)	71

[a] Yield is based on weights of powder and crystalline material combined. [b] Commercial filings. [c] 3 h at 60 °C, and stirred overnight at room temperature. [d] The yield and solubility calculations for these compounds were based on the compositions indicated by elemental analyses for **6a** and **6b** $[M(NCS)_2(NCMe)_x]$ (M = Ca, x = 2; M = Yb, x = 2.5).

$[Eu(NCS)_3(dme)_{2.5}]_2$ (1c): *rac*-**4c** (0.22 g, 0.41 mmol) was isolated as a yellow powder and added with $Hg(SCN)_2$ (0.070 g, 0.20 mmol) to a Schlenk flask which was subsequently charged with dme (30 mL) and stirred at ambient temperature for 3 d resulting in the precipitation of elemental mercury. The reaction mixture was allowed to settle and then was filtered through a filter cannula. The filtrate was concentrated to 4 mL and stored at 5 °C until one large yellow block-shaped crystal appeared which was suitable for study by X-ray crystallography; m.p. 178–181 °C (dec. 268 °C). IR (Nujol): $\tilde{\nu}$ = 2069 (sh), 2050 (vs) cm^{-1}. 2038 sh, 2004 sh, 1282 w, 1241 m, 1186 m, 1111 w, 1093 s, 1038 vs, 1020 sh, 1008 sh, 981 w, 902 m, 864 s, 856 s, 827 w, 782 w, 574 w. $C_{13}H_{25}Eu_1N_3O_5S_3$ (551.50): calcd. Eu 27.55; found Eu 28.13.

$[Dy(NCS)_3(dme)_{2.5}]_2$ (1d): The pale yellow filtrate was concentrated to 2 mL followed by the addition of 1 mL of toluene. Storage at 5 °C of the Schlenk flask placed in a horizontal position afforded small colourless plate-shaped crystals; m.p. 132–136 °C. IR (Nujol): $\tilde{\nu}$ = 2074 (sh), 2054 (vs), 2045 (sh), 2009 (sh), 1280 (vw), 1243 (w), 1186 (w), 1112 (w), 1094 (m), 1039 (vs), 1020 (sh), 1007 (sh), 983 (vw), 905 (w), 868 (m), 860 (m), 829 (vw), 783 (vw) cm^{-1}. $C_{13}H_{25}Dy_1N_3O_5S_3$ (562.04): calcd. Dy 28.91, NCS 31.00; found Dy 28.59, NCS 29.77.

$[Er(NCS)_3(dme)_{2.5}]_2$ (1e): The pink filtrate was concentrated until it gave a greasy appearance (2 mL) and 1 mL of toluene was added. The Schlenk flask was stored in a horizontal position at 5 °C until pink rod-shaped crystals deposited; m.p. 178–181 °C. IR (Nujol): $\tilde{\nu}$ = 2078 (sh), 2058 (vs), 2046 (sh), 2013 (sh), 1280 (vw), 1243 (w), 1186 (w), 1113 (w), 1094 (s), 1038 (vs), 1020 (sh), 1008 (sh), 985 (vw), 905 (m), 869 (s), 861 (s), 830 (vw), 782 (vw) cm^{-1}. $C_{13}H_{25}Er_1N_3O_5S_3$ (566.80): calcd. C 27.54, H 4.46, N 7.41 Er 30.54; found C 26.80, H 4.48, N 7.19, Er 29.51.

$[Yb(NCS)_3(dme)_2]$ (1f): $[Yb(NCS)_2(thf)_2]$ was prepared according to the literature procedure[14] by treating freshly filed Yb metal with $Hg(SCN)_2$ in thf. $[Yb(NCS)_2(thf)_2]$ (0.20 g. 0.46 mmol) was isolated as a red powder then combined with $Hg(SCN)_2$ (0.073 g, 0.23 mmol) in a Schlenk flask. Dme (30 mL) was added to the powders resulting in a dark green solution. Upon stirring for less than 1 min, elemental mercury deposited as a black precipitate and the solution became colourless. The reaction mixture was stirred for a further 3 d at room temperature and then allowed to stand. The mercury settled to the bottom of the reaction vessel and the mother liquor was isolated by filtration though a filter cannula. The filtrate was concentrated to saturation (1 mL) followed by the addition of a small volume of toluene (1 mL) and allowed to stand at room temperature. After 1 week, colourless crystalline needles deposited which were suitable for X-ray crystallography; m.p. 180–186 °C. IR (Nujol): $\tilde{\nu}$ = 2062 (sh), 2037 (vs), 1366 (w), 1278 (w), 1259 (vw), 1240 (w), 1189 (w), 1161 (vw), 1110 (w), 1084 (s), 1034 (vs), 868 (m), 859 (s), 826 (w) cm^{-1}. $C_{11}H_{20}N_3O_4S_3Yb_1$ (527.52): calcd. C 25.04, H 3.82, N 7.97; found C 25.72, H 3.83, N 7.92. The metal analysis suggests partial loss of dme from the sample used, calcd. (%) for $C_{10}H_{17.5}N_3O_{3.5}S_3Yb_1$ (505.00, $[Yb(NCS)_3(dme)_{1.75}]$); Yb 34.27 (no dme lost: Yb, 32.80); found Yb 34.23.

$[Er(NCS)_3(diglyme)(dme)]$ (2): $[Er(NCS)_3(dig)(dme)]$ was prepared in a similar way to **1e** except toluene was replaced by diglyme resulting in the deposition of single crystals of **2** in very low yield; m.p. 198–201 °C. IR (Nujol): $\tilde{\nu}$ = 2075 (vs), 2038 (vs), 1287 (w), 1241 (w), 1193 (w), 1111 (m), 1076 (s), 1038 (s), 938 (w), 869 (m), 830 (w), 805 (vw) cm^{-1}. $C_{13}H_{24}ErN_3O_5S_3$ (565.79): calcd. C 27.66, H 4.29, N 7.45; found C 27.71, H 4.23, N 7.37.

thf Complexes of $RE(NCS)_3$

$[Y(NCS)_3(thf)_4]_2$ (3a): The yellow filtrate was concentrated to 10 mL and deposited single colourless block-shaped crystals upon standing at ambient temperature; m.p. 339 °C (dec.). IR (Nujol): $\tilde{\nu}$ = 2104 (vs), 2057 (sh), 2044 (vs), 2000 (s), 1347 (vw), 1296 (w), 1261 (w), 1174 (w), 1097 (w), 1038 (m), 1022 (s), 958 (w), 923 (m), 862 (s), 835 (sh), 803 (w), 673 (m) cm^{-1}. $C_{19}H_{32}N_3O_4S_3Y_1$ (551.57): calcd. Y 16.16; found Y 16.61.

$[La(NCS)_3(thf)_4]_2$ (3b): The yellow filtrate was concentrated to 10 mL and deposited fine needle-shaped colourless crystals upon storage at 5 °C; m.p. 206–208 °C. IR (Nujol): $\tilde{\nu}$ = 2098 (vs), 2039 (sh), 2028 (vs), 1628 (vw), 1341 (w), 1295 (vw), 1248 (w), 1181 (m),

1020 (vs), 979 (m), 955 (m), 921 (m), 863 (s), 854 (sh), 803 (w), 670 (s) cm^{-1}. elemental analysis (fresh crystalline material). $C_{19}H_{32}La_1N_3O_4S_3$ {[$La(NCS)_3(thf)_4]_2$} (601.58): calcd. La 23.09; found La 22.95; calcd. for $C_{16}H_{26}La_1N_3O_{3.25}S_3$ [$La(NCS)_3(thf)_{3.25}$] (547.50), [analysis of stored crystalline material (C,H,N) and powdered product (La)]: calcd. C 35.10, H 4.79, N 7.67, La 25.37; found C 35.17, H 5.16, N 6.87, La 25.68.

[Nd(NCS)$_3$(thf)$_4$]$_2$ (3c): The blue filtrate was concentrated to 10 mL and deposited blue block-shaped crystals upon standing at ambient temperature; m.p. 216–220 °C. IR (Nujol): $\tilde{\nu}$ = 2101 (vs), 2044 (sh), 2032 (vs), 1295 (vw), 1261 (w), 1180 (vw), 1021 (m), 981 (vw), 957 (vw), 922 (w), 863 (m), 845 (sh), 806 (w), 669 (w) cm^{-1}. $C_{19}H_{32}N_3Nd_1O_4S_3$ (606.91): calcd. C 37.60, H 5.31, N 6.92, Nd 23.77; found C 37.25, H 5.27, N 7.11, Nd 24.07.

[Sm(NCS)$_3$(thf)$_4$]$_2$ (3d): The pale yellow filtrate was concentrated to 10 mL and deposited pale yellow block-shaped crystals upon standing at ambient temperature; m.p. 248–252 °C. IR (Nujol): $\tilde{\nu}$ = 2102 (vs), 2046 (vs), 2035 (sh), 1295 (w), 1261 (w), 1247 (w), 1172 (br), 1020 (s), 958 (w), 922 (m), 862 (s), 815 (sh), 800 (vw), 669 (m) cm^{-1}. $C_{19}H_{32}N_3O_4S_3Sm_1$ (613.03): calcd. C 37.23, H 5.26, N 6.85, Sm 24.53; found C 37.11, H 5.23, N 7.04, Sm 24.40.

[Dy(NCS)$_3$(thf)$_4$]$_2$ (3e): The pale yellow filtrate was concentrated to 10 mL and deposited colourless crystalline needles upon storage at 5 °C; m.p. 324–328 °C (dec.). IR (Nujol): $\tilde{\nu}$ = 2103 (s), 2053 (sh), 2042 (vs), 1343 (w), 1295 (w), 1260 (m), 1172 (w), 1095 (m), 1077 (m), 1022 (s), 959 (w), 922 (m), 862 (m), 803 (m), 673 (m) cm^{-1}. $C_{19}H_{32}Dy_1N_3O_4S_3$ (625.17): calcd. Dy 25.99, NCS 27.87; found Dy 25.58, NCS 27.35.

[Ho(NCS)$_3$(thf)$_4$]$_2$ (3f): The pink filtrate was concentrated to ca. 5 mL and the precipitate recrystallised from hot solvent. Large crystals (pink or yellow, depending on light) deposited after a few hours; m.p. 195–200 °C (sweats at 100 °C). IR (Nujol): $\tilde{\nu}$ = 2104 (m), 2043 (s), 1341 (w), 1295 (w), 1172 (m), 1100 (m), 1019 (s), 922 (w), 860 (m), 672 (m) cm^{-1}. $C_{19}H_{32}Ho_1N_3O_4S_3$ (627.59): calcd. Ho 26.28; found Ho 25.55.

[Er(NCS)$_3$(thf)$_4$]$_2$ (3g): Single crystals were grown by recrystallisation of the dme complex **1e** from thf.

Complexes of RE/Ca(NCS)$_2$

[Ca(NCS)$_2$(dme)$_3$] (*rac*-4a): The colourless filtrate was concentrated to 10 mL and stored at 5 °C until colourless block-shaped crystals suitable for X-ray crystallography deposited; m.p. 130–136 °C (dec. 292 °C): IR (Nujol): $\tilde{\nu}$ = 2106 (m), 2061 (vs), 2014 (sh), 1413 (vw), 1363 (m), 1274 (m), 1250 (vw), 1237 (w), 1189 (m), 1156 (w), 1113 (s), 1066 (vs), 1027 (s), 971 (w), 866 (m), 858 (sh), 839 (m), 779 (vw) cm^{-1}. $C_{14}H_{30}CaN_2O_6S_2$ (426.60): calcd. C 39.40, H 7.09, N 6.57; found C 39.70, H 7.22, N 6.79.

[Sm(NCS)$_2$(dme)$_3$] (*rac*-4b): The dark green filtrate was concentrated to 5 mL and stored at 5 °C overnight affording dark green block-shaped single crystals which were analysed by X-ray crystallography; m.p. 58–62 °C (solvent loss), 121 °C (dec. green→yellow), 330 °C (dec. yellow→brown). IR (Nujol): $\tilde{\nu}$ = 2051 (vs), 2004 (m), 1412 (vw), 1274 (m), 1248 (w), 1236 (w), 1202 (w), 1189 (m), 1156 (w), 1114 (s), 1065 (vs), 1027 (m), 1011 (m), 964 (w), 860 (s), 854 (s), 836 (m), 775 (w) cm^{-1}. UV/Vis near IR: (0.024 (M) 616 nm, shoulder at) 428 nm cm^{-1}. $C_{14}H_{30}N_2O_6S_2Sm$ (536.87): calcd. C 31.32, H 5.63, N 5.21; found C 30.77, H 5.64, N 5.42.

[Eu(NCS)$_2$(dme)$_3$] (*rac*-4c/Λ-4c): The yellow/orange filtrate was concentrated to 10 mL and toluene was added (2 mL). The flask was left at ambient temperature until the formation of yellow/orange single yellow plate-shaped crystals one of which was shown by X-ray crystallography to be Λ-**4c**. Further crystallisation from the filtrate was attempted at 5 °C resulting in the crystallisation of one large yellow plate-shaped crystal of *rac*-**4c**. M.p. 126–129 °C (dec. 326 °C). IR (Nujol): $\tilde{\nu}$ = 2059 (vs), 2005 (sh), 1411 (vw), 1283 (w), 1240 (m), 1192 (m), 1160 (w), 1117 (s), 1067 (vs), 1030 (s), 1016 (m), 953 (w), 864 (sh), 855 (s), 842 (m), 774 (w) cm^{-1}. $C_{14}H_{30}EuN_2O_6S_2$ (538.48): calcd. Eu 28.22; found Eu 28.17.

[Ca(NCS)$_2$(dme)$_2$(H$_2$O)] (5): During an attempted crystallization of *rac*-**4a**, crystals of **5** were isolated from a dme solution which had been stored at 5 °C for 2 months. The structure of **5** was determined by single-crystal X-ray crystallography and no further characterisation was attempted.

[Ca(NCS)$_2$(NCMe)$_5$]·NCMe (6a): The colourless filtrate was concentrated to 5 mL and stored at 5 °C causing colourless block-shaped single crystals to deposited which were analysed by single-crystal X-ray crystallography; m.p. 152–158 °C. IR (Nujol): $\tilde{\nu}$ = 2304 (s), 2271 (s), 2100 (vs), 2058 (sh), 2003 (vs), 1962 (sh), 1261 (m), 1160 (vw), 1087 (m), 1031 (s), 990 (w), 954 (w), 933 (sh), 928 (m), 816 (w), 803 (w), 772 (w) cm^{-1}. $C_6H_6Ca_1N_4S_2$ (237.97, only two acetonitrile molecules retained): calcd. C 30.23, H 2.54, N 23.51; found C 29.95, H 2.99, N 22.65.

[Yb(NCS)$_2$(NCMe)$_5$]·NCMe (6b): The dark red filtrate was concentrated to 5 mL followed by the addition of hexane (1 mL). The flask was cooled to –28 °C causing deep red rod-shaped crystalline material to deposit which was suitable for X-ray crystallography; m.p. 179 °C (dec). IR (dark red powder plus crystals): $\tilde{\nu}$ = (Nujol): $\tilde{\nu}$ = 2300 m, 2270 (s), 2054 (vs), 1996 (sh), 1261 (m), 1151 (vw), 1081 (sh), 1030 (m), 931 (vw), 802 (m), 773 (sh) cm^{-1}. elemental analysis of a dark red mixture of crystalline and powdered material calcd. (%) for $C_7H_{7.5}N_{4.5}S_2Yb_1$ (391.84, 2.5 acetonitrile molecules retained): Yb 44.3; found Yb 45.4%; Further drying gave yellow powder. IR (Nujol): $\tilde{\nu}$ = 2300 (vw), 2278 (vw), 2058 (vs), 2006 (sh), 1030 (vw), 974 (w), 789 (vw) cm^{-1}. elemental analysis of yellow powder calcd. (%) for $C_{3.2}H_{1.8}N_{2.6}S_2Yb_1$ (313.83, 0.6 acetonitrile molecules retained): C 12.25, H 0.58, N 11.60; found C 12.32, H 0.89, N 11.61.

[Eu(NCS)$_2$(thf)$_4$]$_2$ (7): The yellow filtrate was concentrated to 5 mL leading to the formation of single yellow/brown block-shaped crystals which were analysed by X-ray crystallography; m.p. > 360 °C. IR (Nujol): $\tilde{\nu}$ = 2119 (vs), 2048 (vs), 2023 (vs), 1260 (w), 1171 (m), 1045 (vs), 891 (m), 804 (w), 772 (vw), 668 (w) cm^{-1}. $C_{18}H_{32}EuN_2O_4S_2$ (556.54): calcd. NCS 20.87; found NCS 20.56.

X-ray General Experimental: Crystalline samples of **1a**–**f**, **2**, **3a**–**g**, *rac*-**4a**–**c**, Λ-**4c**, **5**, **6a**,**b**, and **7** were mounted on glass fibres in viscous hydrocarbon oil at low temperature as specified below. Data for **1a**–**d**, **2a**–**d**, *rac*-**4a**–**c**, Λ-**4c**, **5**, **6a**,**b**, and **7** were collected on a Bruker ApexII diffractometer [equipped with monochromated Mo-K_α radiation (λ = 0.71073 Å) processed by using the SAINT[64] and SADABS[64] package (Bruker)] while **1e**,**f** and **2** data was collected on a Enraf–Nonius Kappa CCD diffractometer (using graphite monochromated Mo-K_α X-ray radiation (λ = 0.71073 Å) where data was corrected for absorption with a SORTAV multi-scan absorption correction[65]). The structures were solved by direct methods, and all reflections were used in least-squares refinement on F^2, with anisotropic thermal parameters refined for non-hydrogen atoms. Hydrogen atoms were placed in calculated positions using a riding model. Structural solution and refinement were carried out using the SHELX suite of programs[66] with the graphical interface X-seed.[67]

CCDC-763903 (for **1a**), -763904 (for **1b**), -763905 (for **1c**), -763906 (for **1d**), -763907 (for **1e**), -763908 (for **1f**), -763909 (for **2**), -763910

(for **3a**), -763911 (for **3b**), -763912 (for **3e**), -763913 (for **3f**), -763914 (for **3g**), -763915 (for **5**), -763916 (for **6a**), -763917 (for **6b**), -763918 (for **7**), -763919 (for Λ-**4c**), -763920 (for *rac*-**4a**), -763921 (for *rac*-**4b**), -763922 (for *rac*-**4c**) contain the supplementary crystallographic data for this paper. These data can be obtained free of charge from The Cambridge Crystallographic Data Centre via www.ccdc.cam.ac.uk/data_request/cif.

1a: $C_{15}H_{30}La_1N_3O_6S_3$ M = 583.51, rod colourless, 0.30 × 0.25 × 0.10 mm^3, monoclinic, $P2_1/c$ (No. 14), a = 11.6415(3), b = 30.5877(7), c = 14.0985(3) Å, β = 90.334(1)°, V = 5020.2(2) Å^3, Z = 8, D_c = 1.544 g/cm^3, F(000) = 2352, T = 123(1) K, $2\theta_{max}$ = 55.0°, 71018 reflections collected, 11530 unique (R_{int} = 0.0283). Final *GooF* = 1.318, *R1* = 0.0376, wR_2 = 0.0727, R indices based on 11388 reflections with $I > 2\sigma(I)$ (refinement on F^2), 519 parameters, 0 restraints.

***Details*:** The crystal structure of (**1a**) was modelled as a pseudo-merohedral twin.[68]

1b: $C_{15}H_{30}N_3Nd_1O_6S_3$ M = 588.84, blue block, 0.08 × 0.05 × 0.05 mm^3, monoclinic, $P2_1/n$ (No. 14), a = 10.3202(2), b = 14.1075(3), c = 17.1523(4) Å, β = 98.291(1)°, V = 2471.14(9) Å^3, Z = 4, D_c = 1.583 g/cm^3, F(000) = 1188, T = 123(1) K, $2\theta_{max}$ = 55.0°, 34753 reflections collected, 5682 unique (R_{int} = 0.0265). Final *GooF* = 1.180, *R1* = 0.0212, wR_2 = 0.0508, R indices based on 5328 reflections with $I > 2\sigma(I)$ (refinement on F^2), 259 parameters, 0 restraints.

1c: $C_{13}H_{25}Eu_1N_3O_5S_3$ M = 551.50, yellow block, 0.18 × 0.07 × 0.07 mm^3, monoclinic, $P2_1/n$ (No. 14), a = 13.9021(3), b = 11.4955(2), c = 14.2134(2) Å, β = 101.198(1)°, V = 2228.22(7) Å^3, Z = 4, D_c = 1.644 g/cm^3, F(000) = 1100, T = 123(1) K, $2\theta_{max}$ = 55.0°, 10649 reflections collected, 4917 unique (R_{int} = 0.0139). Final *GooF* = 1.232, *R1* = 0.0208, wR_2 = 0.0473, R indices based on 4729 reflections with $I > 2(I)$ (refinement on F^2), 231 parameters, 0 restraints.

1d: $C_{13}H_{25}Dy_1N_3O_5S_3$ M = 562.04, colourless plate, 0.15 × 0.13 × 0.07 mm^3, monoclinic, $P2_1/n$ (No. 14), a = 13.8712(3), b = 11.4308(2), c = 14.1864(3) Å, β = 101.309(1)°, V = 2205.71(8) Å^3, Z = 4, D_c = 1.693 g/cm^3, F(000) = 1112, T = 123(1) K, $2\theta_{max}$ = 50.0°, 34852 reflections collected, 3884 unique (R_{int} = 0.0925). Final *GooF* = 1.373, *R1* = 0.0809, wR_2 = 0.1558, R indices based on 3740 reflections with $I > 2\sigma(I)$ (refinement on F^2), 231 parameters, 0 restraints.

1e: $C_{13}H_{25}Er_1N_3O_5S_3$ M = 566.80, pink rod, 0.12 × 0.05 × 0.03 mm^3, monoclinic, $P2_1/n$ (No. 14), a = 13.856(3), b = 11.427(2), c = 14.183(3) Å, β = 101.33(3)°, V = 2201.9(8) Å^3, Z = 4, D_c = 1.710 g/cm^3, F(000) = 1120, T = 123(1) K, $2\theta_{max}$ = 55.0°, 9889 reflections collected, 5655 unique (R_{int} = 0.188). Final *GooF* = 1.027, *R1* = 0.0718, wR_2 = 0.0925, R indices based on 2444 reflections with $I > 2\sigma(I)$ (refinement on F^2), 231 parameters, 0 restraints.

1f: $C_{11}H_{20}N_3O_4S_3Yb_1$ M = 527.52, colourless needle, 0.20 × 0.08 × 0.05 mm^3, monoclinic, space group $P2_1/c$ (No. 14), a = 8.2637(17), b = 15.499(3), c = 15.074(3) Å, β = 95.83(3)°, V = 1920.7(7) Å^3, Z = 4, D_c = 1.824 g/cm^3, F(000) = 1028, T = 123(1) K, $2\theta_{max}$ = 55.0°, 18716 reflections collected, 4414 unique (R_{int} = 0.1596). Final *GooF* = 1.040, *R1* = 0.0735, *wR2* = 0.1659, R indices based on 2819 reflections with $I > 2\sigma(I)$ (refinement on F^2), 203 parameters, 0 restraints.

2: $C_{13}H_{24}ErN_3O_5S_3$, M = 565.79, pink rod, 0.16 × 0.08 × 0.05 mm^3, monoclinic, space group $P2_1/n$ (No. 14), a = 9.5201(19), b = 14.388(3), c = 15.930(3) Å, β = 103.25(3)°, V = 2124.0(7) Å^3, Z = 4, D_c = 1.769 g/cm^3, F(000) = 1116, λ = 0.71073 Å, T = 123(2) K, $2\theta_{max}$ = 55.0°, 17974 reflections collected, 4872 unique (R_{int} = 0.1181). Final *GooF* = 1.072, *R1* = 0.0592, *wR2* = 0.1118, R indices based on 3063 reflections with $I > 2\sigma(I)$ (refinement on F^2), 230 parameters, 0 restraints.

The original $[RE(NCS)_3(thf)_4]_2$ structures reported by Depaoli et al.[11] were assigned to the $P2_1/a$ space group. In this work the space group is assigned as more conventional $P2_1/c$. Unit cell data for **3c** and **3d** at 123 K and of **3g** at room temperature are reported (Table 2).

Table 2. Unit cell data for complexes **3c** and **3d** at 123 K and **3g** at room temperature.

Unit cell data	(**3c**) **Nd**	(**3d**) **Sm**	(**3g**) **Er**
a [Å]	17.340(8)	17.344(9)	17.58(2)
b [Å]	8.025(2)	8.011(5)	8.134(6)
c [Å]	19.197(9)	19.132(9)	18.92(2)
β [°]	112.20(2)	112.05(4)	110.72(2)
Space group	$P2_1/c$	$P2_1/c$	$P2_1/c$
Volume (Å^3)	2471(3)	2463(3)	2533.1(8)

3a: $C_{19}H_{32}N_3O_4S_3Y_1$ M = 551.57, colourless block, 0.22 × 0.10 × 0.10 mm^3, monoclinic, $P2_1/c$ (No. 14), a = 17.2367(7), b = 7.9931(3), c = 18.8895(8) Å, β = 111.765(2)°, V = 2416.97(17) Å^3, Z = 4, D_c = 1.516 g/cm^3, F(000) = 1144, λ = 0.71073 Å, T = 123(1) K, $2\theta_{max}$ = 55.0°, 34444 reflections collected, 5553 unique (R_{int} = 0.0701). Final *GooF* = 1.009, *R1* = 0.0335, wR_2 = 0.0676, R indices based on 4310 reflections with $I > 2\sigma(I)$ (refinement on F^2), 271 parameters, 0 restraints.

3b: $C_{19}H_{32}LaN_3O_4S_3$, M = 601.57, colourless needles, 0.18 × 0.05 × 0.05 mm^3, monoclinic, space group $P2_1/c$ (No. 14), a = 17.4016(8), b = 8.0416(4), c = 19.2833(9) Å, β = 112.205(2)°, V = 2498.3(2) Å^3, Z = 4, D_c = 1.599 g/cm^3, F(000) = 1216, T = 123(1) K, $2\theta_{max}$ = 50.0°, 31178 reflections collected, 4390 unique (R_{int} = 0.0678). Final *GooF* = 1.144, *R1* = 0.0532, *wR2* = 0.1206, R indices based on 3655 reflections with $I > 2\sigma(I)$ (refinement on F^2), 271 parameters, 0 restraints.

3e: $C_{19}H_{32}DyN_3O_4S_3$, M = 625.16, colourless needles, 0.22 × 0.08 × 0.08 mm^3, monoclinic, space group $P2_1/c$ (No. 14), a = 17.2457(4), b = 7.9935(2), c = 18.9293(4) Å, β = 111.822(1)°, V = 2422.48(10) Å^3, Z = 4, D_c = 1.714 g/cm^3, F(000) = 1252, T = 123(1) K, $2\theta_{max}$ = 50.0°, 42197 reflections collected, 4265 unique (R_{int} = 0.0277). Final *GooF* = 1.226, *R1* = 0.0240, *wR2* = 0.0584, R indices based on 4187 reflections with $I > 2\sigma(I)$ (refinement on F^2), 271 parameters, 0 restraints.

3f: $C_{19}H_{32}HoN_3O_4S_3$, M = 627.59, colourless needles, 1.50 × 1.00 × 0.50 mm^3, monoclinic, space group $P2_1/c$ (No. 14), a = 17.2250(3), b = 7.9865(2), c = 18.8930(4) Å, β = 111.797(1)°, V = 2413.24(9) Å^3, Z = 4, D_c = 1.727 g/cm^3, F(000) = 1256, T = 123(1) K, $2\theta_{max}$ = 55.0°, 19605 reflections collected, 5531 unique (R_{int} = 0.0217). Final *GooF* = 1.032, *R1* = 0.0160, *wR2* = 0.0354, R indices based on 5158 reflections with $I > 2\sigma(I)$ (refinement on F^2), 271 parameters, 0 restraints.

3g: $C_{19}H_{32}ErN_3O_4S_3$, M = 629.92, 0.15 × 0.10 × 0.05 mm^3, monoclinic, space group $P2_1/c$ (No. 14), a = 17.2454(6), b = 7.9927(2), c = 18.8699(6) Å, β = 111.700(2)°, V = 2416.65(13) Å^3, Z = 4, D_c = 1.731 g/cm^3, F(000) = 1260, T = 123(2) K, $2\theta_{max}$ = 55.0°, 27163 reflections collected, 5537 unique (R_{int} = 0.0614). Final *GooF* = 1.038, *R1* = 0.0368, *wR2* = 0.0605, R indices based on 4455 reflections with $I > 2\sigma(I)$ (refinement on F^2), 271 parameters, 0 restraints.

***rac*-4a:** $C_{14}H_{30}CaN_2O_6S_2$, M = 426.60, colourless rod, $0.32 \times 0.11 \times 0.11$ mm^3, monoclinic, space group $C2/c$ (No. 15), a = 21.0523(9), b = 8.8692(4), c = 14.8981(11) Å, β = 128.422(2)°, V = 2179.4(2) Å^3, Z = 4, D_c = 1.300 g/cm^3, $F(000)$ = 912, T = 123(1) K, $2\theta_{max}$ = 55.0°, 10338 reflections collected, 2514 unique (R_{int} = 0.0286). Final *GooF* = 1.078, *R1* = 0.0352, *wR2* = 0.0784, R indices based on 2272 reflections with $I > 2\sigma(I)$ (refinement on F^2), 118 parameters, 0 restraints.

***rac*-4b:** $C_{14}H_{30}N_2O_6S_2Sm$, M = 536.87, dark green block, $0.72 \times 0.51 \times 0.29$ mm^3, monoclinic, space group $C2/c$ (No. 15), a = 20.9843(5), b = 8.9632(2), c = 14.7961(3) Å, β = 127.953(1)°, V = 2194.39(8) Å^3, Z = 4, D_c = 1.625 g/cm^3, $F(000)$ = 1080, λ = 0.71073 Å, T = 123(1) K, $2\theta_{max}$ = 55.0°, 8426 reflections collected, 2506 unique (R_{int} = 0.0248). Final *GooF* = 1.265, *R1* = 0.0182, *wR2* = 0.0457, R indices based on 2482 reflections with $I > 2\sigma(I)$ (refinement on F^2), 117 parameters, 0 restraints.

***rac*-4c:** $C_{14}H_{30}EuN_2O_6S_2$, M = 538.48, yellow plate, $0.08 \times 0.05 \times 0.03$ mm^3, monoclinic, space group $C2/c$ (No. 15), a = 20.9942(6), b = 8.9605(2), c = 14.7971(5) Å, β = 127.950(2)°, V = 2195.01(11) Å^3, Z = 4, D_c = 1.629 g/cm^3, $F(000)$ = 1084, T = 123(1) K, $2\theta_{max}$ = 50.0°, 12800 reflections collected, 1937 unique (R_{int} = 0.0413). Final *GooF* = 1.107, *R1* = 0.0180, *wR2* = 0.0352, R indices based on 1875 reflections with $I > 2\sigma(I)$ (refinement on F^2), 117 parameters, 0 restraints.

Λ-4c: $C_{14}H_{30}EuN_2O_6S_2$, M = 538.48, yellow plate, $0.10 \times 0.10 \times 0.04$ mm^3, monoclinic, space group $P2_1$ (No. 4), a = 8.4835(2), b = 10.4327(2), c = 13.0076(3) Å, β = 96.153(1)°, V = 1144.62(4) Å^3, Z = 2, D_c = 1.562 g/cm^3, $F(000)$ = 542, T = 123(1) K, $2\theta_{max}$ = 55.0°, 23711 reflections collected, 5240 unique (R_{int} = 0.0282). Final *GooF* = 1.268, *R1* = 0.0198, *wR2* = 0.0395, R indices based on 5183 reflections with $I > 2\sigma(I)$ (refinement on F^2), 232 parameters, 1 restraint. Absolute structure parameter = 0.028(8) (H. D. Flack, *Acta Cryst. A* **1983**, *39*, 876–881).

5: $C_{10}H_{22}CaN_2O_5S_2$, M = 354.50, rod colourless, $0.30 \times 0.20 \times 0.10$ mm^3, monoclinic, space group $P2_1/n$ (No. 14), a = 9.9604(2), b = 15.4793(3), c = 11.6082(2) Å, β = 90.934(1)°, V = 1789.51(6) Å^3, Z = 4, D_c = 1.316 g/cm^3, $F(000)$ = 752, T = 123(2) K, $2\theta_{max}$ = 55.0°, 32369 reflections collected, 4093 unique (R_{int} = 0.0251). Final *GooF* = 1.156, R_1 = 0.0265, wR_2 = 0.0604, R indices based on 3919 reflections with $I > 2\sigma(I)$ (refinement on F^2), 269 parameters, 0 restraints.

6a: $C_{14}H_{18}CaN_8S_2$, M = 402.56, colourless plate, $0.05 \times 0.05 \times 0.02$ mm^3, orthorhombic, space group *Pbcn* (No. 60), a = 9.7134(1), b = 23.3299(4), c = 9.62310(10) Å, V = 2180.72(5) Å^3, Z = 4, D_c = 1.226 g/cm^3, $F(000)$ = 840, T = 123(2) K, $2\theta_{max}$ = 50.0°, 29551 reflections collected, 1921 unique (R_{int} = 0.0246). Final *GooF* = 1.263, R_1 = 0.0374, wR_2 = 0.0907, R indices based on 1908 reflections with $I > 2\sigma(I)$ (refinement on F^2), 121 parameters, 1 restraint.

6b: $C_{14}H_{18}N_8S_2Yb$, M = 535.52, yellow block, $0.06 \times 0.04 \times 0.04$ mm^3, orthorhombic, space group *Pbcn* (No. 60), a = 9.7156(2), b = 23.3458(5), c = 9.6502(2) Å, V = 2188.84(8) Å^3, Z = 4, D_c = 1.625 g/cm^3, $F(000)$ = 1040, T = 123(2) K, $2\theta_{max}$ = 55.0°, 29111 reflections collected, 2526 unique (R_{int} = 0.0290). Final *GooF* = 1.314, *R1* = 0.0265, *wR2* = 0.0436, R indices based on 2419 reflections with $I > 2\sigma(I)$ (refinement on F^2), 121 parameters, 0 restraints.

7: $C_{18}H_{32}EuN_2O_4S_2$, M = 556.54, yellow block, $0.25 \times 0.25 \times 0.20$ mm^3, monoclinic, space group $P2_1/c$ (No. 14), a = 15.5246(7), b = 15.1656(7), c = 10.3807(5) Å, β = 95.371(2)°, V = 2433.3(2) Å^3, Z = 4, D_c = 1.519 g/cm^3, $F(000)$ = 1124, T = 210(2) K, $2\theta_{max}$ = 50.0°, 58680 reflections collected, 4284 unique (R_{int} = 0.0275). Final *GooF* = 1.252, *R1* = 0.0312, *wR2* = 0.0514, R indices based on 4168 reflections with $I > 2\sigma(I)$ (refinement on F^2), 428 parameters, 97 restraints.

Details: All thf molecules were disordered but were modelled successfully over two positions. The geometries of the five membered rings were restrained to be reasonable. Further restraints were added for the anisotropic refinement of the disordered atoms.

Supporting Information (see also the footnote on the first page of this article): Selected bond lengths and angles for all structures (Tables S1a, S2–S9), and a comparison of dme ligand positions for **1a**,**b** (Table S1b), structural diagrams for compounds **2** (Figure S2a), **3e**, representative of **3a**–**3g** (Figure S4), **5** (Figure S6), **6b** (Figure S7), specific orientations of coordination spheres of **1c**–**e** (Figure S1), *rac*-**4a**–**c** (Figure S6), **7** (Figure S9) and packing diagrams for **2** (Figure S3) and **6a**,**b** (Figure S8).

Acknowledgments

We are grateful to the Australian Research Council and Monash University for funding and to the Monash Research Graduate School for the provision of a postgraduate scholarship (J. M. B). M. W. thanks the Deutsche Forschungsgemeinschaft for a research fellowship.

[1] F. T. Edelmann, *Comprehensive Organometallic Chemistry III*, vol. 4, Elsevier, **2007**; F. T. Edelmann, D. M. M. Freckmann, H. Schumann, *Chem. Rev.* **2002**, *102*, 1851; T. J. Boyle, L. A. M. Ottley, *Chem. Rev.* **2008**, *108*, 1896; H. Schumann, J. A. Meese-Marktscheffel, L. Esser, *Chem. Rev.* **1995**, *95*, 865; R. C. Mehrotra, A. Singh, U. M. Tripathi, *Chem. Rev.* **1991**, *91*, 1287; R. Anwander, *Top. Curr. Chem.* **1996**, *179*, 33; F. A. Hart, *Comprehensive Coordination Chemistry*, vol. 3 (Eds.: G. Wilkinson, R. D. Gillard, J. A. McCleverty), Pergamon, Oxford, **1987**, pp. 1059; F. T. Edelmann, *Synthetic Methods of Organometallic and Inorganic Chemistry (Herrmann/Brauer) Lanthanides and Actinides*, vol. 6, Thieme, New York, **1997**; S. Cotton, *Comprehensive Coordination Chemistry II*, vol. 3 (Eds.: J. A. McCleverty, T. J. Meyer, G. F. R. Parkin), Elsevier, Oxford, **2004**, chapter 3.2.

[2] S. Mishra, *Coord. Chem. Rev.* **2008**, *252*, 1996, and references cited therein.

[3] P. Miranda, J. Zukerman-Schpector, P. C. Serrano, G. Vicentini, L. B. Zinner, *J. Alloys Compd.* **2004**, *374*, 358; C. A. De Simone, E. E. Castellano, C. A. Fantin, L. B. Zinner, G. Vicentini, *Lanthanide Actinide Res.* **1987**, *2*, 127; X.-H. Bu, W. Weng, J.-R. Li, W. Chen, *Inorg. Chem.* **2002**, *41*, 413.

[4] S. A. Cotton, V. Franckevicius, R. E. How, B. Ahrens, L. L. Ooi, M. F. Mahon, P. R. Raithby, S. J. Teat, *Polyhedron* **2003**, *22*, 1489.

[5] M. I. Saleh, A. Salhin, B. Saad, S. M. Zain, Z. Arifin, *J. Mol. Struct.* **1997**, *415*, 71.

[6] F. Benetello, G. Bombieri, W. A. Gootee, K. K. Fonda, K. M. Samaria, L. M. Vallarino, *Polyhedron* **1998**, *17*, 3633.

[7] G. Bombieri, F. Benetello, A. Polo, L. De Cola, W. T. Hawkins, L. M. Vallarino, *Polyhedron* **1989**, *8*, 2157.

[8] F. Benetello, G. Bombieri, L. M. Vallarino, *Acta Crystallogr., Sect. C* **1996**, *52*, 1190; F. Benetello, G. Bombieri, G. Depaoli, M. R. Truter, *Inorg. Chim. Acta* **1996**, *245*, 223; J.-G. Mao, Z.-S. Jin, J.-Z. Ni, *Jiegou Huaxue* **1994**, *13*, 329.

[9] F. Benetello, G. Bombieri, K. M. Samaria, L. M. Vallarino, *J. Chem. Crystallogr.* **1996**, *26*, 9.

[10] K. Rossmanith, *Monatsh. Chem.* **1962**, *93*, 1121.

[11] G. Depaoli, P. Ganis, P. L. Zanonato, G. Valle, *Polyhedron* **1993**, *12*, 671.

[12] C. Wickleder, *Z. Anorg. Allg. Chem.* **2001**, *627*, 1693.

[13] G. Depaoli, P. Ganis, P. L. Zanonato, G. Valle, *Polyhedron* **1993**, *12*, 1933.
[14] G. B. Deacon, C. M. Forsyth, D. L. Wilkinson, *Chem. Eur. J.* **2001**, *7*, 1784.
[15] T. Gröb, K. Harms, K. Dehnicke, *Z. Anorg. Allg. Chem.* **2001**, *627*, 125.
[16] P. Nockemann, B. Thijs, N. Postelmans, K. Van Hecke, L. Van Meervelt, K. Binnemans, *J. Am. Chem. Soc.* **2006**, *128*, 13658; B. Mallick, B. Balke, C. Felser, A.-V. Mudring, *Angew. Chem. Int. Ed.* **2008**, *47*, 7635.
[17] F. Matsumoto, N. Matsumura, A. Ouchi, *Bull. Chem. Soc. Jpn.* **1989**, *62*, 1809; N. Matsumura, A. Ouchi, *Kidorui* **1988**, *12*, 146.
[18] A. F. Waters, A. H. White, *Aust. J. Chem.* **1996**, *49*, 27.
[19] J. F. Bower, S. A. Cotton, J. Fawcett, R. S. Hughes, D. R. Russell, *Polyhedron* **2003**, *22*, 347.
[20] Z. Xu, Y. Gu, Q. Zheng, F. Shen, C. Yao, S. Yan, G. Wang, *Wuli Xuebao* **1982**, *31*, 956; C. Huang, R. Xu, X. Xu, G. Xu, *Wuji Huaxue* **1985**, *1*, 103; R. P. Feazell, J. B. Gary, J. A. Kautz, K. K. Klausmeyer, C. W. Wong, M. Zancanella, *Acta Crystallogr., Sect. E* **2004**, *60*, m532.
[21] M. C. Favas, D. L. Kepert, *Prog. Inorg. Chem.* **1981**, *28*, 309; R. S. De Biasi, *J. Mater. Sci.* **1987**, *22*, 4108.
[22] M. Johnson, J. C. Taylor, G. W. Cox, *J. Appl. Crystallogr.* **1980**, *13*, 188.
[23] R. D. Shannon, *Acta Crystallogr., Sect. A* **1976**, *32*, 751.
[24] M. I. Saleh, A. Salhin, B. Saad, H.-K. Fun, *J. Mol. Struct.* **1999**, *475*, 93.
[25] S. G. Zhang, J. M. Shi, *Acta Crystallogr., Sect. E* **2007**, *63*, m1763.
[26] J. Marcalo, A. Pires de Matos, *Polyhedron* **1989**, *8*, 2431.
[27] D. L. Kepert, *Prog. Inorg. Chem.* **1978**, *24*, 179.
[28] J. Liu, E. A. Meyers, J. A. Cowan, S. G. Shore, *Chem. Commun.* **1998**, 2043.
[29] S. Yan, Z. Jiang, D. Liao, G. Wang, R. Wang, H. Wang, X. Yao, *J. Inclusion Phenom. Mol. Recognit. Chem.* **1993**, *15*, 159.
[30] G. Wang, S. Yan, X. Yao, *Sci. Sin., Ser. B (Chim. Ed.)* **1985**, 387.
[31] K. A. Thiakou, V. Nastopoulos, A. Terzis, C. P. Raptopoulou, S. P. Perlepes, *Polyhedron* **2006**, *25*, 539.
[32] M. N. Bochkarev, I. L. Fedushkin, A. A. Fagin, T. V. Petrovskaya, J. W. Ziller, R. N. R. Broomhall-Dillard, W. J. Evans, *Angew. Chem. Int. Ed. Engl.* **1997**, *36*, 133.
[33] D. E. Hibbs, C. Jones, A. F. Richards, *J. Chem. Crystallogr.* **1999**, *29*, 1107.
[34] S. Beaini, G. B. Deacon, M. Hilder, P. C. Junk, D. R. Turner, *Eur. J. Inorg. Chem.* **2006**, 3434.
[35] G. B. Deacon, E. E. Delbridge, G. D. Fallon, C. Jones, D. E. Hibbs, M. B. Hursthouse, B. W. Skelton, A. H. White, *Organometallics* **2000**, *19*, 1713.
[36] D. M. Barnhart, D. L. Clark, J. C. Huffman, R. L. Vincent, J. G. Watkin, *Inorg. Chem.* **1993**, *32*, 4077.
[37] J. E. Cosgriff, G. B. Deacon, G. D. Fallon, B. M. Gatehouse, H. Schumann, R. Weimann, *Chem. Ber.* **1996**, *129*, 953.
[38] T. Gröb, G. Seybert, W. Massa, K. Dehnicke, *Z. Anorg. Allg. Chem.* **2000**, *626*, 349.
[39] a) H. Schumann, K. Herrmann, S. H. Mühle, D. Deckert, *Z. Anorg. Allg. Chem.* **2003**, *629*, 1184; b) H. Schumann, K. Herrmann, J. Demtschuk, S. H. Mühle, *Z. Anorg. Allg. Chem.* **1999**, *625*, 1107; c) J. H. Melman, C. Rohde, T. J. Emge, J. G. Brennan, *Inorg. Chem.* **2002**, *41*, 28.
[40] See, for instance: G. B. Deacon, P. I. MacKinnon, T. W. Hambley, J. C. Taylor, *J. Organomet. Chem.* **1983**, *259*, 91; G. B. Deacon, T. Feng, B. W. Skelton, A. H. White, *Aust. J. Chem.* **1995**, *48*, 741.
[41] M. Hakansson, M. Vestergren, B. Gustafsson, G. Hilmersson, *Angew. Chem. Int. Ed.* **1999**, *38*, 2199.
[42] Y. Y. Wei, B. Tinant, J. P. Declercq, M. Van Meerssche, J. Dale, *Acta Crystallogr., Sect. C* **1987**, *43*, 1076.
[43] A. N. Chekhlov, *Russ. J. Gen. Chem.* **2004**, *74*, 721.
[44] G. B. Deacon, E. E. Delbridge, B. W. Skelton, A. H. White, *Eur. J. Inorg. Chem.* **1999**, 751.
[45] J. Hitzbleck, A. Y. O'Brien, C. M. Forsyth, G. B. Deacon, K. Ruhlandt-Senge, *Chem. Eur. J.* **2004**, *10*, 3315.
[46] S. Westhusin, P. Gantzel, P. J. Walsh, *Inorg. Chem.* **1998**, *37*, 5956.
[47] T. Gröb, G. Seybert, W. Massa, K. Harms, K. Dehnicke, *Z. Anorg. Allg. Chem.* **2000**, *626*, 1361.
[48] W. J. Evans, R. N. R. Broomhall-Dillard, J. W. Ziller, *Polyhedron* **1998**, *17*, 3361.
[49] T. Gröb, G. Seybert, W. Massa, K. Dehnicke, *Z. Anorg. Allg. Chem.* **1999**, *625*, 1897.
[50] Y. Y. Wei, B. Tinant, J. P. Declercq, M. Van Meerssche, J. Dale, *Acta Crystallogr., Sect. C* **1987**, *43*, 1080.
[51] K. M. Fromm, H. Goesmann, G. Bernardinelli, *Polyhedron* **2000**, *19*, 1783.
[52] D. Belli Dell'Amico, C. Bradicich, L. Labella, F. Marchetti, *Inorg. Chim. Acta* **2006**, *359*, 1659.
[53] W. H. Watson, D. A. Grossie, F. Vögtle, W. M. Müller, *Acta Crystallogr., Sect. C* **1983**, *39*, 720.
[54] W. J. Evans, T. S. Gummersheimer, J. W. Ziller, *J. Am. Chem. Soc.* **1995**, *117*, 8999.
[55] P. W. Roesky, *Inorg. Chem.* **2006**, *45*, 798.
[56] T. D. Tilley, A. Zalkin, R. A. Andersen, D. H. Templeton, *Inorg. Chem.* **1981**, *20*, 551.
[57] J. H. Melman, T. J. Emge, J. G. Brennan, *Inorg. Chem.* **2001**, *40*, 1078.
[58] J. Hitzbleck, A. Y. O'Brien, G. B. Deacon, K. Ruhlandt-Senge, *Inorg. Chem.* **2006**, *45*, 10329.
[59] G. Heckmann, M. Niemeyer, *J. Am. Chem. Soc.* **2000**, *122*, 4227.
[60] C. M. Forsyth, G. B. Deacon, *Organometallics* **2000**, *19*, 1205.
[61] A. H. Norbury, *Adv. Inorg. Chem. Radiochem.* **1975**, *17*, 231.
[62] a) K. Nakamoto, *Infrared Spectra of Inorganic and Coordination Compounds*, 2nd ed., John Wiley & Sons, New York, **1970**; b) A. M. Golub, H. Kohler, V. V. Skopenko, *Thiocyanate compounds*, in: *Chemistry of Pseudohalides*, vol. 21 (Ed.: R. J. H. Clark), Elsevier, New York, **1985**, pp. 279.
[63] J. Lewis, J. R. Miller, R. L. Richards, A. Thompson, *J. Chem. Soc.* **1965**, 5850.
[64] *SAINT* and *SADABS* are part of the ApexII software package, Bruker AXS, Madison, WI, USA.
[65] R. H. Blessing, *Acta Crystallogr., Sect. A* **1995**, *51*, 33.
[66] G. M. Sheldrick, *SHELXL-97*, University of Göttingen, Germany, **1997**; G. M. Sheldrick, *SHELXS-97*, University of Göttingen, Germany, **1997**.
[67] L. J. Barbour, *J. Supramol. Chem.* **2003**, *1*, 189.
[68] P. Müller, R. Herbst-Irmer, A. L. Spek, T. R. Schneider, M. R. Sawaya, *Crystal Structure Refinement A Crystallographer's Guide to SHELXL*, Oxford University Press, Oxford, **2006**.

Received: February 1, 2010
Published Online: March 31, 2010

